EXPLORATORY RESEARCH

sesar JOINT UNDERTAKING

FlyATM4E

Report on final results on eco-efficient trajectories

Deliverable ID:	**D3.2**
Dissemination Level:	**PU**
Project Acronym:	**FlyATM4E**
Grant:	**891317**
Call:	**H2020-SESAR-2019-2**
Topic:	**SESAR-ER4-05-2019 Environment and Meteorology for ATM**
Consortium Coordinator:	**DLR**
Edition date:	**19 August 2022**
Edition:	**00.02.00**
Template Edition:	**02.00.05**

EUROPEAN PARTNERSHIP

Co-funded by the European Union

Authoring & Approval

Authors of the document

Name / Beneficiary	Position / Title	Date
Federica Castino (TUD)	WP3 contributor	08/07/2022
Benjamin Lührs (DLR)	WP2 Contributor	08/07/2022
Maximilian Mendiguchia Meuser (TUHH)	WP2 Contributor	08/07/2022
Abolfazl Simorgh (UC3M)	WP2 Contributor	08/07/2022

Reviewers internal to the project

Name / Beneficiary	Position / Title	Date
Simone Dietmüller (DLR)	WP1 contributor	22/06/2022
Feijia Yin (TUD)	WP3 Leader	08/07/2022
Maximilian Mendiguchia Meuser (TUHH)	WP2 Contributor	18/08/2022

Approved for submission to the SJU By - Representatives of all beneficiaries involved in the project

Name / Beneficiary	Position / Title	Date
Feijia Yin (TUD)	WP3 Leader	18/08/2022
Sabine Baumann (DLR)	Deputy Coordinator	19/08/2022
Manuel Soler (UC3M)	WP4 Leader	18/08/2022
Maximilian Mendiguchia Meuser (TUHH)	WP2 Contributor	18/08/2022

Document History

Edition	Date	Status	Name / Beneficiary	Justification
00.00.01	24/03/2022	Initial Draft	Federica Castino (TUD)	New document
00.00.02	29/03/2022	Complete Draft	Federica Castino (TUD)	WP3 internal review
00.00.10	31/03/2022	Submitted Draft	Federica Castino (TUD)	Reviewed document
00.00.11	17/05/2022	Updated Draft	Federica Castino (TUD)	Updated document
00.00.12	08/07/2022	Complete Report	Federica Castino (TUD)	Internal review
00.01.00	08/07/2022	Submitted Report	Federica Castino (TUD)	Final version
00.01.01	16/08/2022	Updated Report	Federica Castino (TUD)	SJU comments
00.02.00	19/08/2022	Submitted Report	Federica Castino (TUD)	Reviewed document

EUROPEAN PARTNERSHIP

Co-funded by the European Union

FlyATM4E

FLYING AIR TRAFFIC MANAGEMENT FOR THE BENEFIT OF ENVIRONMENT AND CLIMATE

This Report is part of a project that has received funding from the SESAR Joint Undertaking under grant agreement No 891317 under European Union's Horizon 2020 research and innovation programme.

Abstract

The objective of this Deliverable is to describe the final results obtained within the Work Package 3 (WP3) of the FlyATM4E project towards the identification of "eco-efficient" aircraft solutions, i.e. trajectories and respective meteorological situations which allow a substantial reduction in the climate impact of a flight with low - or without - penalties in fuel consumption and operating costs.

To this end, we further developed the AirTraf and ACCF submodels, which are coupled with the ECHAM/MESSy Atmospheric Chemistry (EMAC) model. This modelling chain allows us to compute feasible trade-offs between climate impact and aircraft operating costs on a yearly time-scale, thus considering the natural variability of atmospheric conditions. In particular, we optimized an air traffic sample of 100 European flights for day-time and night-time separately, and we identified eco-efficient trajectories within the set of Pareto-optimal solutions. Moreover, inefficiency in the system was taken into account to identify "win-win" solutions, reducing both cost and climate impact. For this task, we compared the results from ROOST, a model which optimizes trajectories on a structured-airspace (using the current network of Air Traffic Services routes), to the results from TOM, an optimization tool that uses free-routing airspace (future concept of operations).

The achievements documented in this deliverable contribute to the overall project objective O3 on how to identify aircraft trajectories and related weather situations, enabling: (1) "eco-efficient" solutions, which largely reduce the climate impact of aviation at almost unchanged costs; or (2) "win-win" situations, which have the potential to reduce both climate impact and operational costs.

Table of Contents

List of Tables

EUROPEAN PARTNERSHIP

Co-funded by the European Union

List of Figures

EUROPEAN PARTNERSHIP

Co-funded by the European Union

1 Introduction

This report presents the final results obtained within the Work Package 3 (WP3) of the FlyATM4E project towards the identification of "eco-efficient" aircraft solutions, i.e., trajectories and respective meteorological situations which allow a substantial reduction in the climate impact of a flight with low - or without - penalties in fuel consumption and operating costs.

In Section 1 we describe the problem context and the WP3 objectives. Subsequently, we present the methods used in WP3, including the model developments that have been implemented during the FlyATM4E project. Section 3 presents the results of the simulations conducted with the newly developed model setup, which will be further analysed in the last period of the project. In Section 4, we highlight our main findings, and we include our view on the next steps that are needed in this research field.

1.1 Background

The contribution of air traffic to global warming is due to CO_2 and non-CO_2 effects, including the impact of NO_x emissions on atmospheric ozone and methane, formation of contrails, and emission of water vapour. Non-CO_2 effects from aviation operate on shorter time scales than the perturbation from CO_2 emissions; as a consequence, the climate impact of non-CO_2 effects is highly dependent on the background atmospheric conditions at the time and location of emission [12]. This dependency results in the potential to mitigate the climate impact of aviation by optimizing the aircraft trajectories [21].

Previous projects (e.g., REACT4C [9], ATM4E [12]) evaluated the mitigation potential of aircraft trajectories optimization under representative weather patterns. By simulating the impact of air traffic with an Earth System Model, it was found that a 25% reduction in the climate impact of westbound trans-Atlantic flights could be achieved with a ~0.5% increase in the operational costs on a representative winter day [8].

To further explore this mitigation potential, the FlyATM4E project aims to analyse optimal aircraft trajectories in the European airspace under various weather situations. To this end, the air traffic submodel AirTraf [25] is coupled with the ECHAM/MESSy Atmospheric Chemistry (EMAC [10]) model: this allows for optimizing an air traffic sample over long simulation periods (i.e., one year or longer), thus considering a large number of weather patterns. As a balance of computational effort, the impacts of flight routes on networks are idealized. For example, the cost model assumes a linear dependence between costs of time and time of flight to represent the costs due to longer working hours and usage of the airplane; this assumption neglects extra costs due to delay time/route charges (see Section 2.1.3). Therefore, air traffic complexity is out of scope in FlyATM4E.

Moreover, by comparing cost-optimal trajectories computed on a structured-airspace (using the current network of Air Traffic Services routes) with climate-optimal trajectories computed on a free-routing airspace (future concept of operations), we explored the possibility of identifying win-win solutions in which both cost and climate impact could be reduced. The optimization tools used for this task will be the ROOST and TOM model (see Section 2.2), which are selected to simulate a structured and free-routing airspace, respectively.

EUROPEAN PARTNERSHIP

Co-funded by the European Union

1.2 Objectives of WP3

In the WP3 of the FlyATM4E project, we aim to achieve the following objectives:

1. To identify *eco-efficient* solutions, i.e., trajectories and respective meteorological situations which allow a substantial reduction in the climate impact of a flight while leaving its cost nearly unchanged (Figure 1a);

2. To identify *win-win* situations, in which optimized trajectories enable to reduce both climate impact and cost (Figure 1b).

In particular, the objective is to identify these *eco-efficient* and *win-win* situations in the European Airspace.

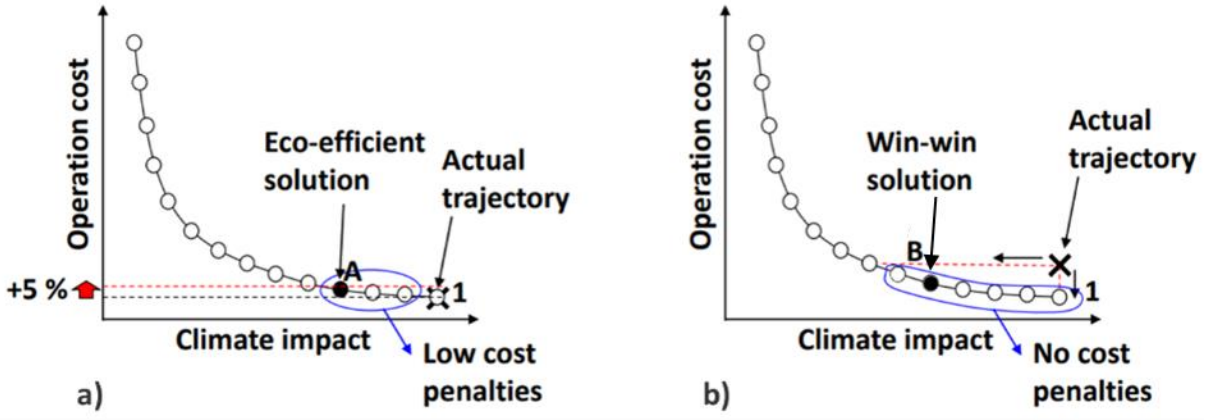

Figure 1 - Schematic illustration of the WP3 objectives: identification of eco-efficient (a) and win-win (b) solutions. The blue circles indicate the set of solutions that allow for a reduction in the climate impact at low cost penalties (a) or without cost penalties (b).

EUROPEAN PARTNERSHIP

Co-funded by the European Union

2 Methods

This section describes the methodologies used to identify “eco-efficient” and “win-win” solutions, defined in Section 1.2.

2.1 Identification of “eco-efficient” solutions

To analyse eco-efficient solutions, we conducted simulations over one year with the air traffic simulator AirTraf coupled to the chemistry model EMAC. During the FlyATM4E project, we completed the following model developments:

1. We implemented the educated guess prototype algorithmic Climate Change Functions (aCCFs) provided by the FlyATM4E Work Package 1 (see Deliverable D1.2 [28]) in the ACCF submodel;

2. We implemented a new Multi-Objective Optimization Module, including Decision-Making methods, in the AirTraf submodel to identify “eco-efficient” flights.

These model developments are described in more detail in Section 2.1.2 and Section 2.1.3, respectively. AirTraf V3.0 optimizes the trajectories taking into account their impact on the climate, estimated using the EMAC submodels ACCF V1.0 and CONTRAIL V1.0. Figure 2 shows the overview of the model chain and how different elements interact. Such a model chain allows us to run long-term simulations to investigate the role of weather parameters in obtaining the “eco-efficient” solutions. This section elaborates on the modelling procedure.

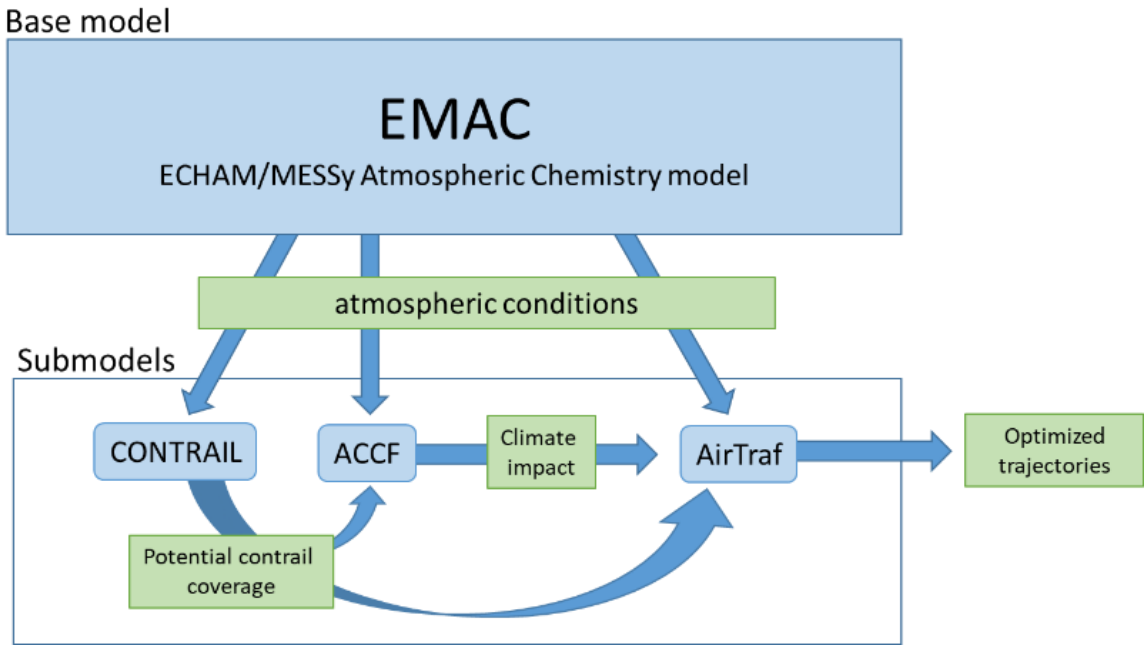

Figure 2 - Overview of the interactions between the base model EMAC and the submodels CONTRAIL, ACCF, and AirTraf (blue boxes). Green boxes represent the input/output of the different components.

EUROPEAN PARTNERSHIP

Co-funded by the European Union

2.1.1 Base model: EMAC

The ECHAM/MESSy Atmospheric Chemistry (EMAC) model is a numerical chemistry and climate simulation system that includes sub-models describing tropospheric and middle atmosphere processes and their interaction with oceans, land, and human influences [10]. It uses the second version of the Modular Earth Submodel System (MESSy2) to link multi-institutional computer codes. The core atmospheric model is the 5th generation European Centre Hamburg general circulation model (ECHAM5, [20]). For the present study, we applied EMAC (ECHAM5 version 5.3.02, MESSy version 2.55.0) in the T42L31ECMWF resolution, i.e., with a spherical truncation of T42 (corresponding to a quadratic Gaussian grid of approx. 2.8 by 2.8 degrees in latitude and longitude) with 31 vertical hybrid pressure levels up to 10 hPa. The duration of the simulation has been set to 1 year, from 1 December 2017 to 1 December 2018. The meteorological conditions simulated by a free-running atmospheric model can differ from the weather patterns that actually occurred during the reference period. An alternative to free-running simulations are 'nudged' simulations, which are performed while keeping some model variables close to the reference atmospheric conditions. In our experiments, the simulations are nudged down to the surface towards the ECMWF ERA-Interim reanalyses data [3]. Table 1 summarizes the configuration of the EMAC model.

Table 1 – Configuration of the base model EMAC for "eco-efficient" flight simulations.

Horizontal resolution	T42 (approx. 2.8 by 2.8 degrees)
Vertical resolution	L31ECMWF (31 vertical pressure levels up to 10 hPa, approx. 30 km)
Time step	20 min
Duration	1 year (from 1 Dec. 2017 to 1 Dec. 2018)

2.1.2 ACCF submodel

The ACCF V1.0 submodel contains the full set of aCCFs formulas developed in the previous ATM4E project to predict the ATR20 from individual effects: NO_x-O3, NO_x-CH4, contrails, CO_2, and H_2O. During the course of the FlyATM4E project, the ACCF submodel [26] has been updated in order to implement the new set of prototype aCCFs provided by WP1 (see Deliverables D1.2 [28]). The new aCCFs formulations, for the first time, provide a consistent set of aCCFs in terms of emission scenarios (pulse or future emission scenario), the efficacy of individual effect, and the educated guess factor to represent the relative importance of the individual effect. The educated guess factors were derived by comparing the results from the ACCF submodel and the AirClim model [2][7]. Please see the details of the prototype aCCFs in Section 3.3 and Appendix A of Deliverable D1.2 of FlyATM4E [28]. The ACCF submodel provides the option to convert from ATR20 of a Pulse emission (P-ATR20) to a different metric, for example, to account for an increasing future emission scenario (F-ATR20). Moreover, the user can choose to include additional factors to consider the efficacy of different climate impacts. The simulations presented in this Deliverable D3.2 include efficacy terms and express the climate impact in terms of ATR20 for a Business As Usual (BAU) future emission scenario – indicated as F-ATR20 in the following text.

EUROPEAN PARTNERSHIP

Co-funded by the European Union

2.1.3 AirTraf submodel

We use the EMAC submodel AirTraf V3.0 [25] to optimize the air traffic under a multitude of weather patterns. AirTraf optimizes aircraft routes based on the atmospheric fields calculated online by the base model EMAC. Please note that AirTraf V3.0 only considers the cruise phase of the flight. The optimization is performed by a genetic algorithm (ARMOGA, [24]), which provides the coordinates of 8 control points: 3 pairs of coordinates along the projection on the Earth, and 5 points in the vertical cross section (varying between FL290 and FL410, corresponding to about 8.8 - 12.5 km). These control points are employed to calculate the flight trajectory, which is represented by a B-spline curve. This resulting B-spline curve is divided into 100 segments (i.e., 101 waypoints), to calculate the properties of each flight along its trajectory.

The input to the AirTraf submodel includes the description of the air traffic sample, indicating the coordinates of the origin/destination pairs and the departure time of each flight. In our simulations, the air traffic sample has been provided by the WP2 (for more details, see D2.2 [29]) using the following main criteria:

1. Be representative for the European air traffic: to this end, an analysis of the European air traffic has been performed, and the top 100 routes by Available Seat Kilometres (ASK) for the European Civil Aviation Conference (ECAC) area in 2018 have been selected. The location of the origin/destination pairs is indicated in Figure 3. Moreover, the A320-214 (CFM56-5B4) aircraft type was selected, based on the total traffic share in ASK for ECAC in 2018.

2. Enable to identify seasons/times of the day which are more likely to present conditions allowing for eco-efficient trajectories: to make this possible, the same origin/destination pairs are repeated on each simulation day at two fixed departure times (00:00, 12:00).

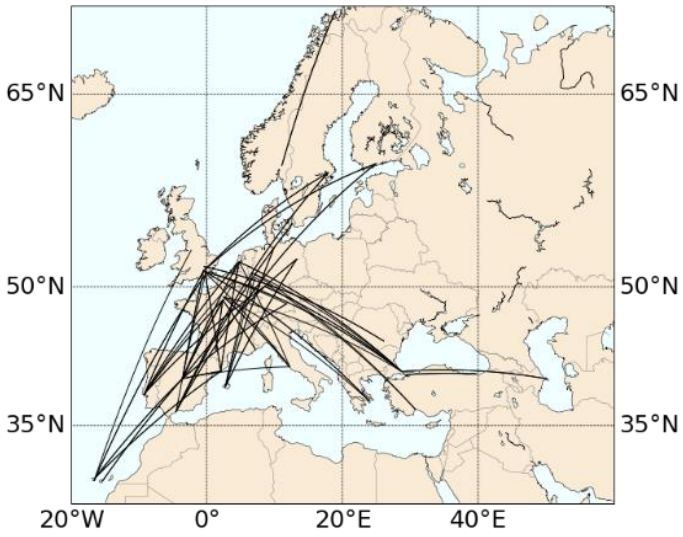

Figure 3 - Location of the 100 origin/destination pairs included in our representative European air traffic sample.

Co-funded by the European Union

2.1.3.1 Objective functions

The optimization module of AirTraf V3.0 includes several objective functions. In this document, we focus on the optimization of the following quantities:

1. Total climate impact, measured as the F-ATR20 (ATR20 for increasing emission scenario in future). The total F-ATR20 is the sum of the main contributors to the aviation climate impact, i.e., day/night contrails, NO_x, CO_2, and H_2O, which are estimated in terms of ATR20 by the ACCF submodel:

$$ATR20_{\text{tot}} = \lambda_{cont}\, ATR20_{cont} + \lambda_{\text{NOx-O3}}\, ATR20_{\text{NOx-O3}} + \lambda_{\text{NOx-CH4}}\, ATR20_{\text{NOx-CH4}} + \lambda_{\text{CO2}}\, ATR20_{\text{CO2}} + \lambda_{H2O}\, ATR20_{\text{H2O}}$$

   where $\lambda_{cont} = 0.42$, $\lambda_{\text{NOx-O3}} = 1.37$, $\lambda_{\text{NOx-CH4}} = 1.18$, $\lambda_{\text{CO2}} = 1.0$, and $\lambda_{\text{H2O}} = 1.0$ represent the efficacy of contrails, NO_x-ozone, NO_x-methane, CO_2, and water vapour effects, respectively [13].

2. Simple Operating Costs (SOC), which are defined as:

$$SOC = c_t \sum_{i=1}^{wp-1} TIME_i + c_f \sum_{i=1}^{wp-1} FUEL_i$$

   where $wp = 101$ are the number of waypoints in which the model divides each trajectory; $c_t\ [\$/s] = 0.75$ \$/s and $c_f\ [\$/kg] = 0.51$ \$/kg represent the unit time cost and the unit fuel cost, respectively [1][25]. The time cost index considers the cost of the flight crew, cabin crew, and maintenance for the airframe and engine.

Using the SOC as objective function, we consider both flight time and fuel use in the optimization process, as the previous studies showed that fuel-optimal trajectories differ from cost-optimal solutions [25]. The definition of SOC assumes a linear dependence between costs of time and time of flight, to represent the costs due to longer working hours and usage of the airplane. As a result, extra costs due to delay time/route charges are not taken into account, as a linear relationship would not be able to represent these penalties. A detailed assessment of the regional strongly varying route charges and their influence on operating costs is beyond the scope of this study.

2.1.3.2 New Optimization Module and Decision-Making options

The AirTraf submodel has been expanded during the FlyATM4E project to enable the resolution of multi-objective optimization problems. As a result, we are able to compare *cost*-optimal (minimum SOC)*, climate-optimal* (minimum F-ATR20) *and eco-efficient* trajectories (feasible trade-off solutions resulting from the simultaneous optimization of the SOC and F-ATR20). The following Multi-Criteria Decision-Making methods have been implemented in the new AirTraf submodel:

- Option 1: the model selects the solution within the set of Pareto-optimal solutions that is closest to an $x\%$ increase in the "preferred" objective (SOC in this study), with respect to its minimum value (located at one of the extreme points of the Pareto set).

EUROPEAN PARTNERSHIP

Co-funded by the European Union

- Option 2: the VIKOR method is applied, using geometric considerations to identify a trade-off solution between the two objectives (in our case, SOC and F-ATR20). Appendix A describes this technique.

The two Decision-Making methods, as they are applied in the simulations presented in this report, are illustrated in Figure 4. In our problem, we are interested in the trade-offs between climate impact (x-axis) and costs (y-axis). Figure 4(a) shows that, with 'Option 1', the cost-optimal solution is used as a reference point to find the closest solution to an $x\%$ increase in costs. On the other hand, with 'Option 2' (Figure 4(b)) a point outside of the Pareto front, representing an 'ideal solution' (minimum costs, minimum climate impact) is used as a reference to find an 'eco-efficient' solution.

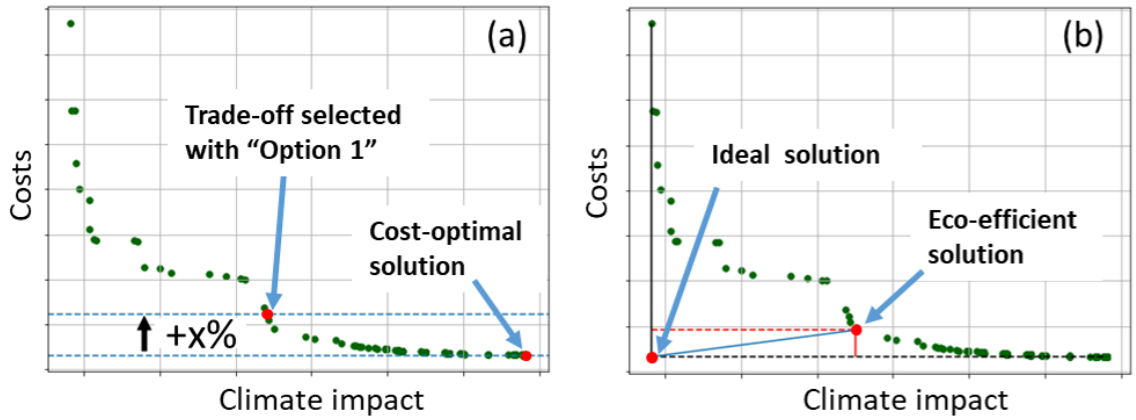

Figure 4 – Overview of the two Decision-Making methods implemented in AirTraf V3.0.

These solution-picking methods have been implemented in AirTraf V3.0, and tests have been performed under the following AirTraf settings:

- Trajectories are identified by solving a bi-objective optimization problem, minimizing F-ATR20 and SOC.
- Different solution-picking options are compared:
  - Option 1 is applied to select those **trade off-solutions** leading to a +0.5% increase in SOC;
  - Option 2 is applied to identify **eco-efficient solutions.**

The results of these simulations contribute to demonstrating the successful implementation of the new version of the AirTraf submodel, and are presented in Section 3 of this report.

2.2 Identification of "win-win" situations

Current aircraft routings are restricted by structured airspace, which is represented by the network of Air Traffic Service routes as well as further additional constraints such as the flight level system. These restrictions cause inefficiencies in both climate impact as well as operating costs in comparison to an unconstrained free-routing solution. Therefore, we intend to find "win-win" solutions in which both

operating costs and climate impact could be reduced in free-routing airspace in comparison to the current structured airspace system (also see Figure 1b).

In order to investigate “win-win” solutions, two tools are applied: Robust Optimization Of STructured airspace (ROOST), which is designed for the optimization of aircraft trajectories in structured airspace, as well as the Trajectory Optimization Module (TOM), which is capable of performing a continuous optimization in vertical and horizontal space.

In the following, an overview of TOM and ROOST is given (see Sections 2.2.1 and 2.2.2) and the simulation setup is described (see Section 2.2.3).

2.2.1 Trajectory Optimization Module (TOM)

For the estimation of continuously optimized trajectories with regard to climate impact and costs, the Trajectory Optimization Module (TOM) is applied. The workflow applied within TOM is illustrated in Figure 5 and briefly described in the following. A more detailed description of TOM is given in D2.1, D2.2 and [14][15].

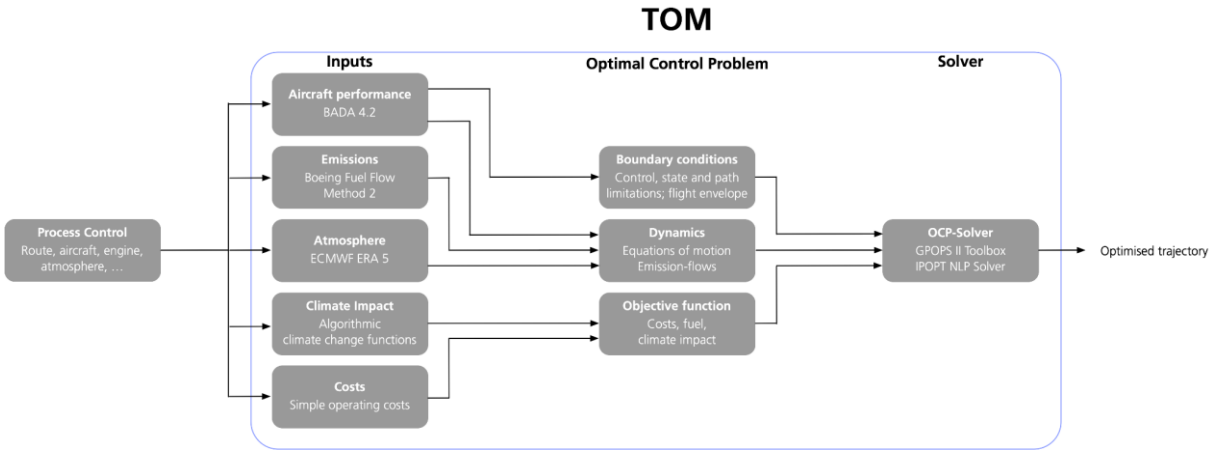

Figure 5 - Workflow applied within the Trajectory Optimization Module.

Process control

TOM consists of an outer loop that is used in order to define the optimization problem and its boundaries. Within the process control, e.g., route, aircraft type, engine type as well as atmospheric conditions are defined. The process control is also used in order to define parameter variations, e.g., a varying cost functional in order to reflect different weights for climate impact and costs.

Inputs

Within TOM, several interfaces to external input data are established. TOM considers aircraft performance data from Eurocontrol’s Base of Aircraft Data (BADA), which is used in order to determine the performance characteristics, including the fuel burn along the optimized trajectory [18]. Emissions are calculated by applying the Boeing Fuel Flow Method 2, and atmospheric data (e. g. wind, temperature, pressure) is taken from the ERA5 dataset of the European Centre of Medium Range

EUROPEAN PARTNERSHIP
Co-funded by the European Union

Weather forecasts (ECMWF) which also contain the necessary atmospheric data which is required for the evaluation of aCCFs which have been further developed in the course of FlyATM4E [4]. The operating costs are estimated as Simple Operating Costs, which are defined as a weighted sum of flight time and fuel burn (see Section 2.1.3.1).

Optimal control problem

Within TOM, the optimization problem is formulated as a continuous optimal control problem which consists of boundary conditions (e.g., limitation of the aircraft's flight envelope) and the dynamics of the optimization problem represented by the equations of motion of the aircraft as well as the emission flows. Additionally, the cost function of the optimization is defined as the weighted sum of climate impact and operating costs.

Solver

The optimization problem is solved by transferring the continuous optimal control problem into a discrete non-linear programming problem using a dedicated toolbox and corresponding NLP solvers.

2.2.2 Robust optimization of structured airspace (ROOST)

Robust optimization of structured airspace (ROOST) is a fast graph-based optimization algorithm suitable for the currently structured airspace (see Figure 5 for an illustration), in which aircraft's states such as lateral path and flight altitude are constrained [6][22].

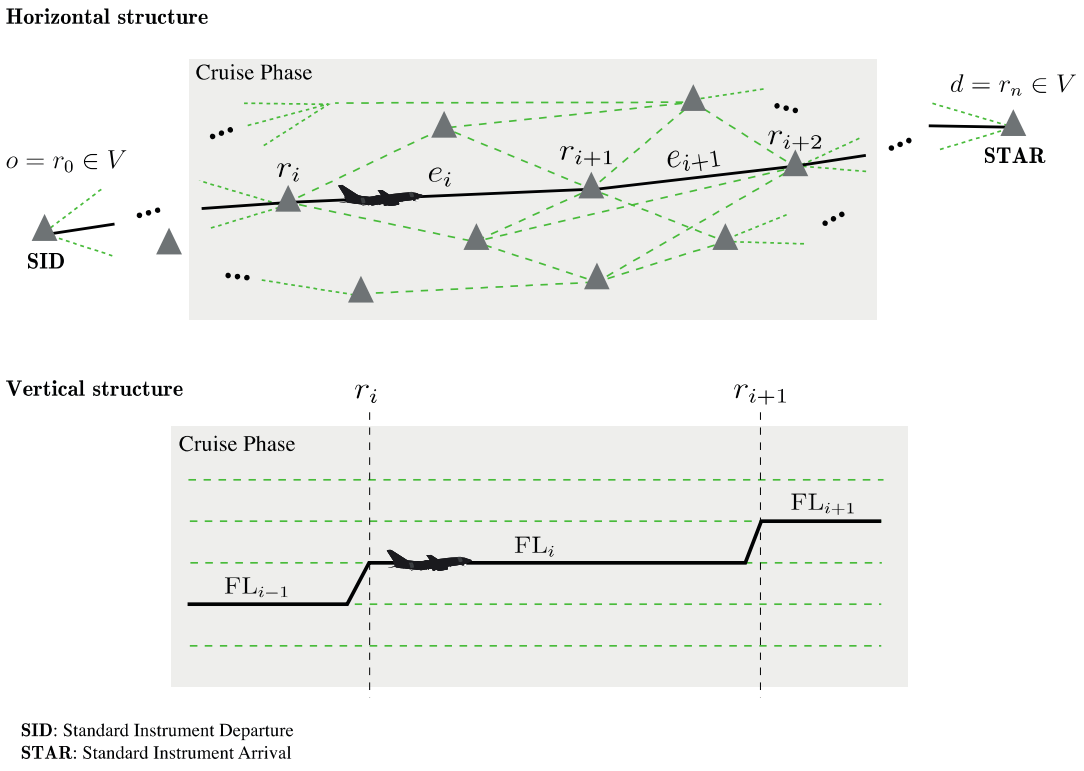

Figure 6 - Airspace structure considered within ROOST.

EUROPEAN PARTNERSHIP
Co-funded by the European Union

For the route graph considered for the case studies included in D2.1 and D2.2 and also analysing the win-win situation in D3.2, the full airspace graph of the selected days is filtered and processed to include all paths starting at the end of the departure procedure and ending at the beginning of the arrival procedure to the destination airport with the maximum length of 104% of the shortest path.

The aircraft dynamical model, boundary conditions, and objective function are defined similarly to the ones considered within TOM (also see Section 2.2.3). As the optimization problem is constrained by the structure of airspace, it is associated with hybrid decision spaces (e.g., route or the flight level are discrete; others, such as the speed schedule or the fuel load, are continuous instead). To account for discrete and continuous decision variables in an integrated manner, the optimization is performed on the space of probability distributions defined over flight plans instead of directly searching for the optimal profile. A heuristic algorithm based on the augmented random search is employed and implemented on graphics processing units to solve the resulting stochastic optimization computationally fast. Detailed descriptions of the methodology can be found in D2.1, D2.2, and [6][22].

2.2.3 Simulation set-up

Since TOM requires a large amount of computational effort, the number of routes to be analysed is restricted. Since the aim is to identify “win-win” situations considering the currently structured airspace, a simplification using “fictitious” routes as proposed in D2.1 is not possible due to the necessity of considering the actual air traffic services route network. Therefore, nine routes of the full real route network estimated within D2.1 which cover a large area over Europe have been considered and are illustrated in Figure 7.

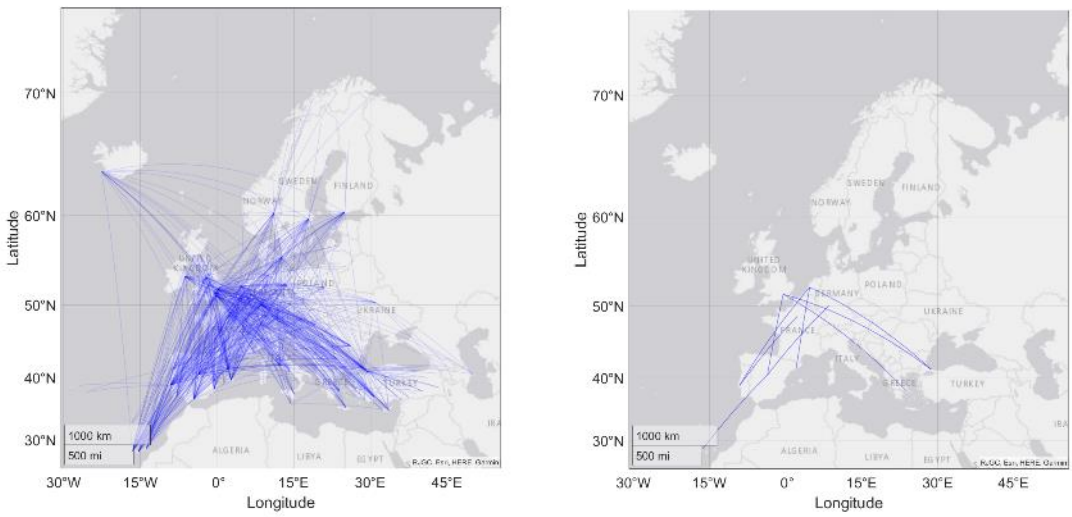

Figure 7 - Route network of the Top 2000 flights of the full traffic scenario from D2.1 (left) and selected routes for the win-win analysis (right).

In addition to the definition of the route network which is considered in the course of the “win-win” situation analysis, additional boundary conditions and assumptions within ROOST and TOM need to be

Co-funded by the European Union

harmonised amongst the tools. A summary of the essential assumptions which have been used in order to ensure comparability of the results is shown in Table 2 -

Table 2 - Boundary conditions in order to ensure comparability of TOM and ROOST results.

Route network	Nine routes, see Figure 7 (right)
Weather situation	2018-12-05, 00:00 UTC, Ensemble 1
Climate impact estimation	Algorithmic climate change functions
Aircraft performance	BADA 4.2 / A320-214
Initial mass	69,300 kg (90% MTOW)
Initial and final pressure altitude	10.000 ft
Initial and final calibrated airspeed	250 knots
Initial and final latitude/longitude	SID / STAR entry/exits
Cost model	Simple Operating Costs (see Section 2.1.3.1)
Cost functional	Weighted sum of climate impact and costs

For all nine routes, the Pareto-fronts (climate impact reduction versus increase in operating costs) are estimated by varying the weights of climate impact and operating costs within the cost functional for both the TOM simulations (continuous) as well as the ROOST simulations (structured airspace).

Co-funded by the European Union

3 Results

3.1 Identification of eco-efficient trajectories

In this section, we describe the results of the long-term simulations that we conducted with the EMAC model, coupled with AirTraf V3.0 and ACCF V1.0 submodels, to optimize the air traffic sample with respect to different optimization objectives. In particular, we compare the F-ATR20 and SOC that characterize four trajectory optimization strategies: (1) cost-optimal, (2) climate-optimal, (3) trade-off solutions, leading to a +0.5% cost increase for each flight, and (4) eco-efficient trajectories, selected by a flexible decision making algorithm.

3.1.1 Mitigation potential

Comparing eco-efficient and cost-optimal trajectories, we found that an increase of about 0.5% in operating costs allows to reduce the climate impact of day-time flights by about 20%, and the impact of night-time flights by about 10%, in terms of F-ATR20.

Figure 8 compares the changes in SOC and F-ATR20 with respect to cost-optimal trajectories, which were obtained employing three different optimization strategies: climate-optimal (green), +0.5% SOC (red), and eco-efficient (blue). The percentages shown in Figure 8 are calculated comparing the total SOC and F-ATR20 values found summing over all the flights and days included in our simulations. Firstly, we can notice that the total increase in SOC obtained with the "fixed +0.5% SOC" solution-picking strategy is lower than the target, i.e., the SOC change is +0.44% instead of +0.5%. This is motivated by the fact that, in some situations, the maximum SOC increase in the Pareto front is lower than the target +0.5% (this will be further discussed in Section 3.1.2). This fact lowers the actual SOC change to +0.44%, both for day-time and night-time flights.

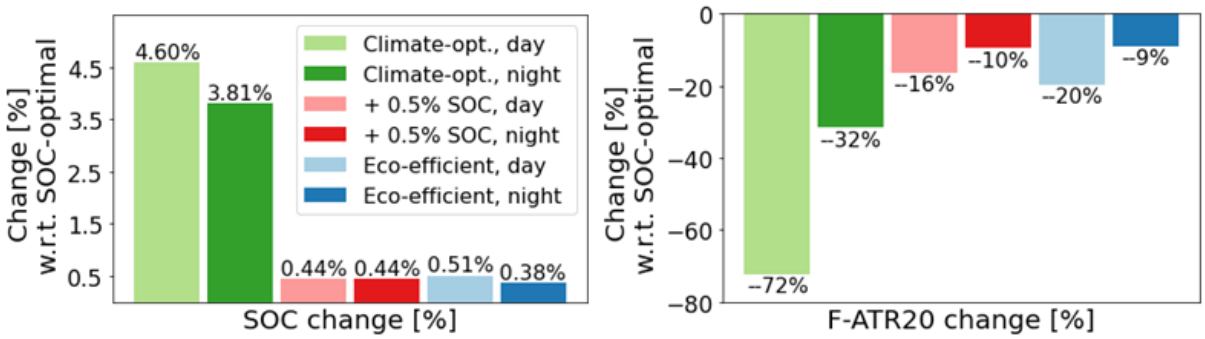

Figure 8 – Relative changes [%] in SOC and F-ATR20 with respect to SOC-optimal trajectories.

Looking at the solutions selected with the fixed +0.5% SOC increase (Option 1 in Section 2.1.3.2) and eco-efficient solutions (Option 2 in Section 2.1.3.2), we can see that a direct comparison of these different solution-picking strategies is difficult, as larger SOC changes correspond to larger F-ATR20 reductions. A method to compare these strategies is suggested in Section 3.1.6.

EUROPEAN PARTNERSHIP

Co-funded by the European Union

Figure 8 also compares the mitigation potential of day-time flights (bars in lighter colours) and night-time flights (bars in darker colours). We can see that the reductions in climate impact are larger during the day, than they are during the night. In particular, the F-ATR20 reduction of climate-optimal trajectories during the day is more than double the night-time mitigation potential, while the SOC increase is less than double. This suggests that there is a higher potential for eco-efficiency during the day, than during the night (we will quantify and compare this difference in Section 3.1.6). The higher mitigation potential of day-time flights is not only visible for climate-optimal trajectories, but also for trade-off solutions, for which the same increase in SOC (+0.44%) leads to a larger F-ATR20 reduction (-16% during the day vs. -10% at night). A possible interpretation for this day-time higher mitigation potential is that, during the day, cooling effects from contrail can be exploited by the model to reduce the F-ATR20 values; this point will be further discussed in Sections 3.1.3 and 3.1.4.

3.1.2 Flight characteristics

Figure 9 shows the variability of the median flight altitude over the air traffic sample throughout the year of simulation (from 1 Dec. 2017 to 1 Dec. 2018). We compare SOC-optimal (blue), climate-optimal (orange) and eco-efficient (green) day-time flights. One can notice that cost-optimal trajectories fly at higher altitudes than climate-optimal and eco-efficient trajectories in order to maximise fuel efficiency. Moreover, the cost-optimal flight altitudes are steady throughout the simulation year.

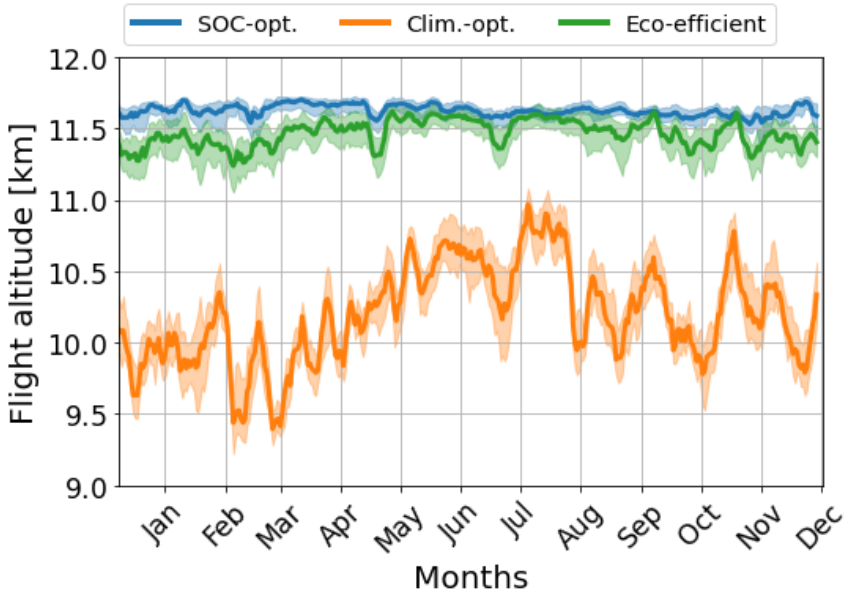

Figure 9 – Mean flight altitude [km] of SOC-optimal (orange), eco-efficient (green), and climate-optimal (orange) day-time flights, with departure time of 12:00 UTC. Bold line: median value over the 100 origin/destination pairs; shaded areas: 1st-3rd quartiles. Note that the values are averaged over each trajectory, and a 7-day running average is applied.

On the other hand, the flight altitudes of climate-optimal are affected by a strong seasonal cycle, as lower altitudes are selected in winter than in summer. This seasonality seems to be present, even if less evident, also for eco-efficient trajectories. The seasonal cycle could be due to the seasonal variability of the tropopause height, which is lower in winter than in summer. This correlation can be

EUROPEAN PARTNERSHIP
Co-funded by the European Union

interpreted considering that, in order to minimize the climate impact of a flight, its emissions should be released at altitudes lower than the tropopause height: this would result in a reduction in the emissions - or the transport of emitted species - in the stratosphere, where the life-time of the emitted species and of their impact on the atmosphere is much larger than in the troposphere [11].

Next, we focus on how the optimization dependent increase in SOC is distributed throughout the simulation year (Figure 10) and over the air traffic sample (Figure 11).

With a flexible distribution of the cost increase over the flights, more resources are allocated in winter (when a daily maximum SOC increase of +1.1% is reached) than in summer (when we find a daily minimum SOC increase below +0.2%).

Figure 10 shows the relative change of the SOC for trade-off flights with respect to the cost-optimal flights. For the trade-off flights, two scenarios are considered: fixed +0.5% SOC increase, and eco-efficient flights. One can see that, as expected, the trajectories with a fixed +0.5% SOC increase lead to a relative change in the operating costs that is approximately constant in time (Figure 10, blue curve), with an average value of +0.44% (Figure 8), slightly below the target of +0.5%. The largest difference from the target SOC increase is found in summer, when a larger fraction of the flights has a maximum SOC increase among the Pareto-optimal solutions which is lower than +0.5%. These results also confirm that the solution-picking method is correctly implemented in the new version of AirTraf (AirTraf V3.0). On the other hand, it is also expected that the relative change in SOC of eco-efficient solutions varies throughout the simulation year, as we can see in Figure 10 (green curve): in winter the SOC increase reaches a maximum (+1.1%), while it is at a minimum in July (+0.17%).

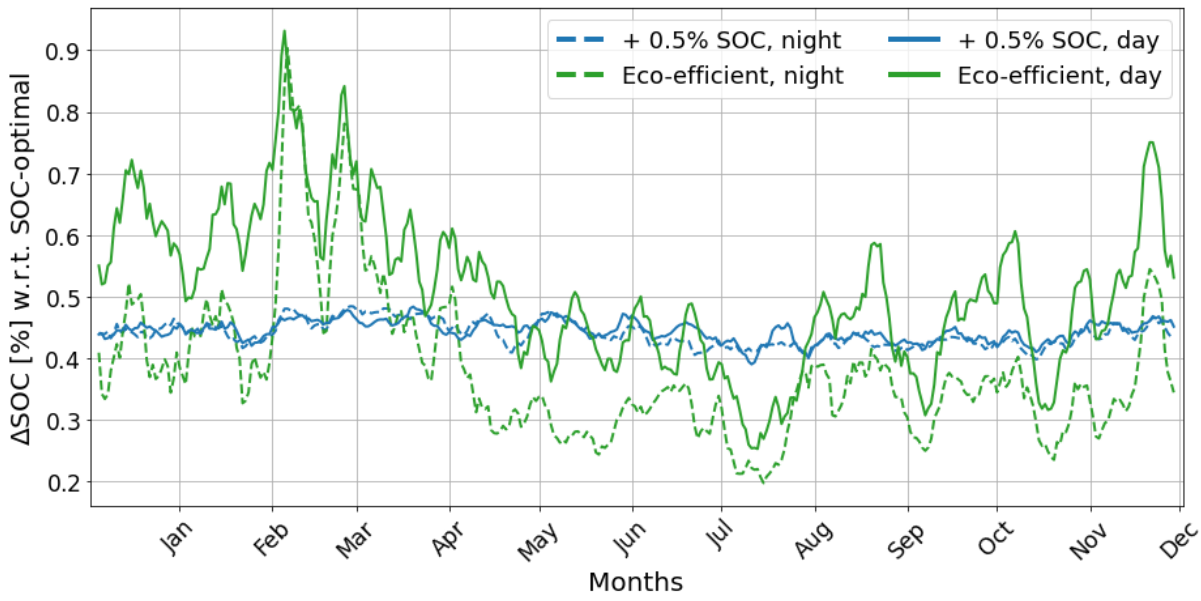

Figure 10 – Relative change [%] in SOC obtained with +0.5% SOC (blue) and eco-efficient (green) trajectories, using as reference the SOC-optimal trajectories. Solid curves: day-time flights (departure time 12:00 UTC); dashed curves: night-time flights (departure time 00:00 UTC). The total change over the air traffic sample (100 flights per day) is shown. The curves show 7-day running mean values.

EUROPEAN PARTNERSHIP

Co-funded by the European Union

Moreover, the cost penalties differ over the flights when different solution-picking strategies are selected, as shown in Figure 11. When the fixed increase in SOC is selected, the curves are centred over the target (see red and orange curves). Eco-efficient solutions have a lower modal value, as most selected flights are close or identical to the cost-optimal options. Larger increases in SOC are allowed in the eco-efficient strategy, but only if these are compensated by a reduction in the climate impact. For a small fraction of the flights (e.g., 3% of night-time eco-efficient trajectories), negative values of the SOC change were obtained from our analysis (not shown in Figure 11), indicating possible inefficiencies in the optimization (i.e., the minimum SOC solution is not always found when the SOC-optimal strategy is applied) or in the post-processing procedures, which are currently being investigated.

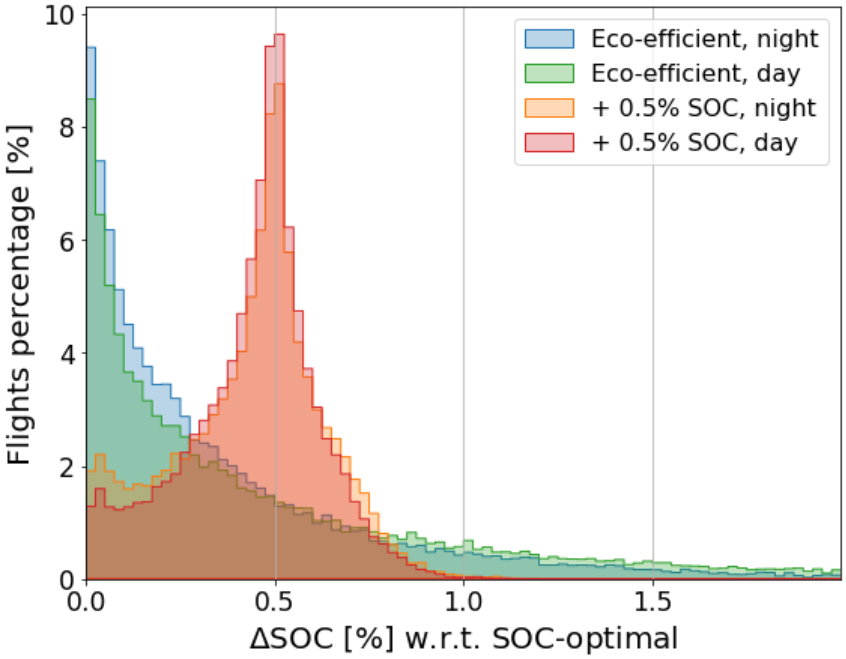

Figure 11 – Histogram showing the percentage of flights characterized by a relative change *x*% in SOC, obtained with the AirTraf eco-efficient solution-picking strategy (blue, green), or the fixed +0.5% SOC strategy (orange, red), using as reference the SOC-optimal trajectories. The flights departure time is 00:00 UTC (blue, orange) or 12:00 UTC (green, red).

3.1.3 Contributions of individual effect

We now describe the difference between climate-optimal and eco-efficient flights for the individual contributions of the aviation climate impact (including CO_2 and non-CO_2 effects).

Changes in contrail effects provide the largest contribution to the reduction in climate impact on almost every day and night – with some exceptions in winter, when the reduction in the F-ATR20 from NO_x-ozone is also contributing. Moreover, in winter, the climate-optimization strategy takes advantage from cooling effects of contrails.

EUROPEAN PARTNERSHIP

Co-funded by the European Union

Figure 12 shows the relative changes in the F-ATR20 [%] of different climate agents from aviation emissions (i.e., CO_2, water vapour, NOx-induced methane and ozone, contrail-cirrus), comparing eco-efficient and cost-optimal day-time flights (baseline). The lower panel includes the changes in the climate impact from contrails, which is the forcing characterized by the largest changes; the total change in F-ATR20 is also shown in the lower panel. The upper panel of Figure 12 includes the remaining climate forcings, which are less affected by changes in the trajectory optimization strategy. One can see that the reductions in contrails and NO_x-ozone are affected by a strong seasonal cycle, with the largest reduction in January and the lowest in June/July. The absolute changes in F-ATR20 [K] between eco-efficient and cost-optimal trajectories are shown in Appendix B (Figure 20-Figure 21): from these figures, we can deduce that the variations in contrail effects represent the largest contribution to the climate impact reduction within the optimization process. The second most important contributor is the reduction in NO_x effects on ozone, which are particularly relevant for night-time flights during winter. Therefore, the seasonal cycle observed in Figure 12 contributes to identifying winter as the season with the largest mitigation potential for day-time flights (see also Figure 15).

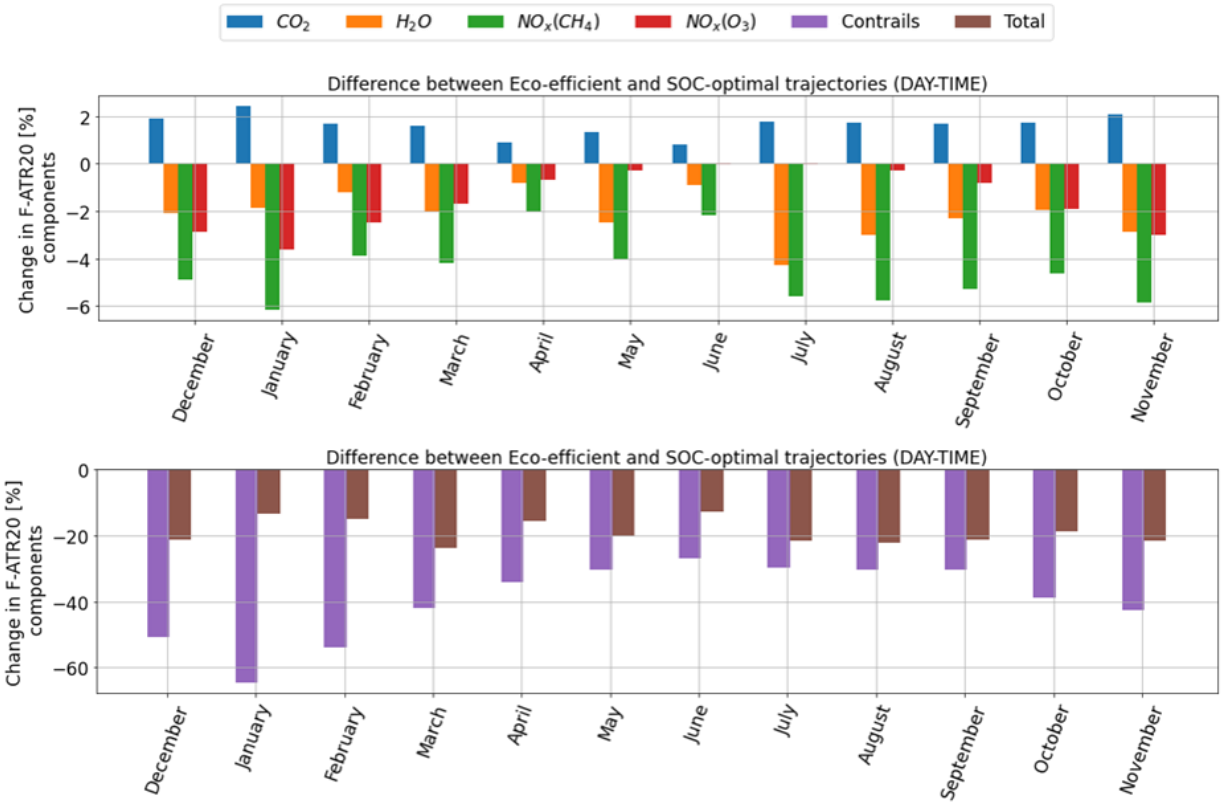

Figure 12 – Relative changes in the F-ATR20 [%] components, relative to the climate impact from different aviation climate forcings, comparing eco-efficient and SOC-optimal trajectories. Upper panel: relative changes in non-dominant effects; lower panel: change in the climate impact of contrails (dominant contributor) and change in total F-ATR20. Departure time of all flights is 12:00 UTC.

EUROPEAN PARTNERSHIP

Co-funded by the European Union

The F-ATR20 of CO_2 is the only term that is always higher for eco-efficient solutions than for cost-optimal trajectories. That is expected, as the climate impact of CO_2 is only dependent on the amount of the emissions and, therefore, it is reduced when the fuel use is minimized.

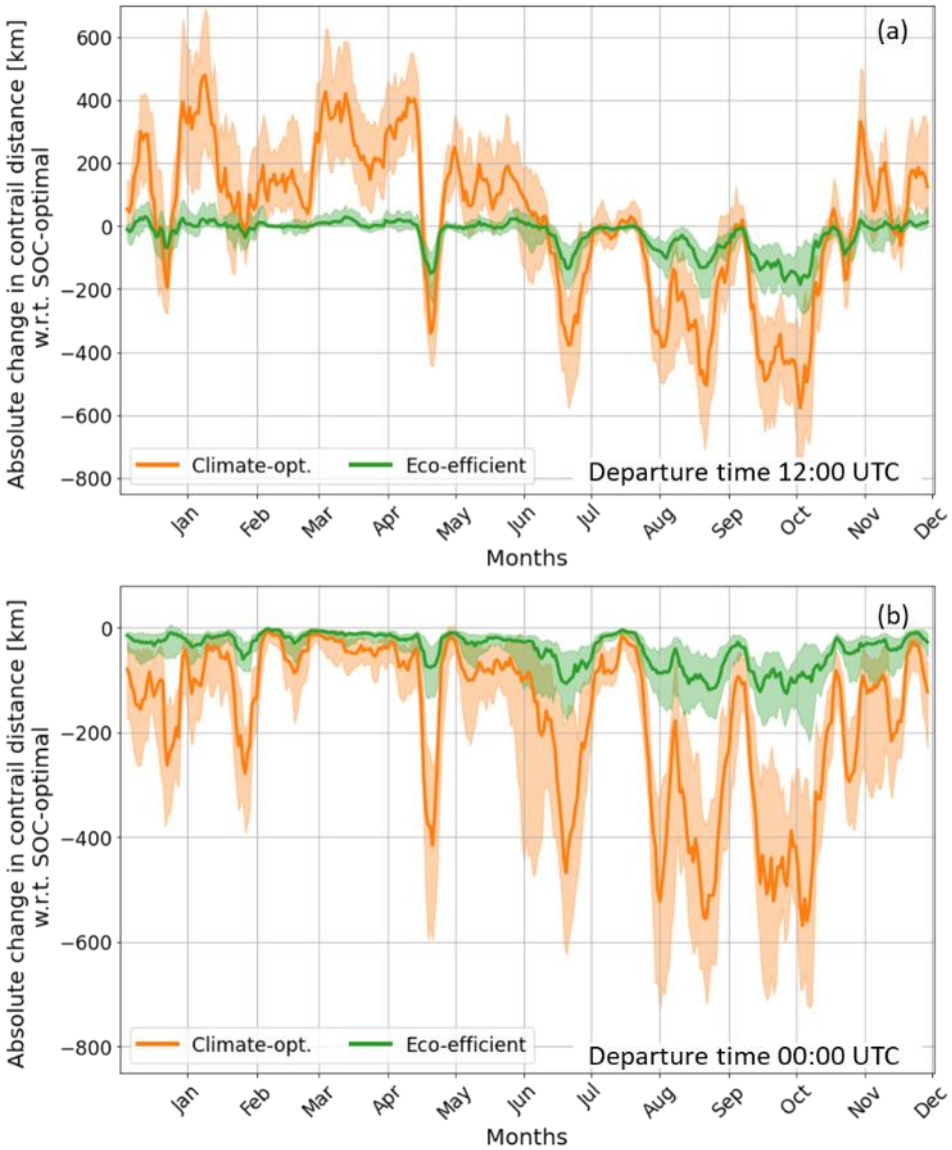

Figure 13 - Absolute change in the contrail distance [km] obtained with the climate-optimal (orange) or with eco-efficient (green) trajectories, using as reference the SOC-optimal trajectories. Bold line: median value over the air traffic sample; shaded areas: 1st-3rd quartiles. Panels (a) and (b) show the results for flights departing at 12:00 and 00:00 UTC, respectively.

We should note that cooling effects from contrails can be used to reduce the F-ATR20 in the trajectory optimization process during the day. We found that this possibility is exploited, especially in winter, when the net F-ATR20 of climate-optimal trajectories can be negative (see Figure 14 and Figure 24). Further research is necessary to understand if eco-efficient trajectories are still leading to higher

EUROPEAN PARTNERSHIP
Co-funded by the European Union

increases in SOC in winter (as shown in Figure 10), and if additional cooling from contrail cannot contribute to the climate impact minimization. This cooling effect is achieved by the formation of contrails that have a negative net radiative forcing. Because of this opportunity, it is possible that more contrails are produced by climate-optimal trajectories than by SOC-optimal ones, as it is shown in Figure 13.

Figure 13 shows the difference in contrail distance [km], i.e., the total flight distance through regions that can be covered by contrails [20]. In fact, contrail distance in climate-optimal trajectories is usually larger in winter, spring, and late autumn (Figure 13(a), orange curve) than for cost-optimal trajectories (baseline). The formation of more contrails in order to lower the climate impact of aviation should be carefully considered, as this may result in a geoengineering intervention. On the other hand, this 'geoengineering' strategy does not dominate in the eco-efficient solutions (Figure 13(a), green curve), since in this scenario, contrail distance is only significantly affected by reductions, in particular during the summer. Nevertheless, it is possible that cooling effects from contrails are still exploited by eco-efficient trajectories in winter since, as we see in Figure 20, changes in contrail F-ATR20 are also in this case the main contributors to the change in the total F-ATR20.

3.1.4 Yearly and diurnal variability of climate impact and mitigation potential

In the following paragraphs, we observe the yearly variability of the total F-ATR20 under different optimization strategies and how it changes between day-time and night-time flights.

The absolute values of the F-ATR20 from our air traffic sample follow a seasonal cycle, with a higher climate impact during the summer (June, July, August), than during the winter (December, January, February). We observe this seasonal cycle under all the trajectory optimization strategies that we considered, i.e., cost-optimal, climate-optimal, and eco-efficient solutions.

From Figure 14, we can observe that the total climate impact from the air traffic sample is subjected to a seasonal cycle. In fact, under all strategies, the F-ATR20 values are on average higher during the summer months, both for day-time and night-time flights. Figure 22-Figure 27 (Appendix B) illustrate the evolution of the F-ATR20 from the different components of aviation's climate impact (contrails, NO_x-ozone, NO_x-methane, H_2O, and CO_2). Figure 22 and Figure 25, which are relative to cost-optimal trajectories, show how the high peaks in F-ATR20 occurring in summer are due to contrail effects. Climate-optimal trajectories successfully avoid contrail effects during the summer season (Figure 24 and Figure 27 in Appendix B), in particular for day-time flights. However, in this scenario, the seasonal cycle is also due to a higher impact from NO_x-ozone effects between June and October, due to higher photochemical activity in this season. Figure 23 and Figure 26, which are relative to eco-efficient trajectories, show that the magnitude of contrails effects is reduced with respect to cost-optimal trajectories (Figure 22 and Figure 25), but the way is varies throughout the year of simulation remains similar to the one of the reference scenario. In Figure 14(a), we can see how the climate optimal-strategy may lead to a negative F-ATR20 during day-time (reached on several days from December 2017 to mid-April 2018), meaning that the net impact of the flights on the environment is a cooling effect. As discussed previously in this section of the report, these negative values are achieved with the formation of more contrails, which may convert our mitigation strategy into a geoengineering

EUROPEAN PARTNERSHIP
Co-funded by the European Union

intervention. For this reason, the next step in this investigation should explore how our results change when we exclude the possibility of exploiting cooling effects from contrails in the optimization process.

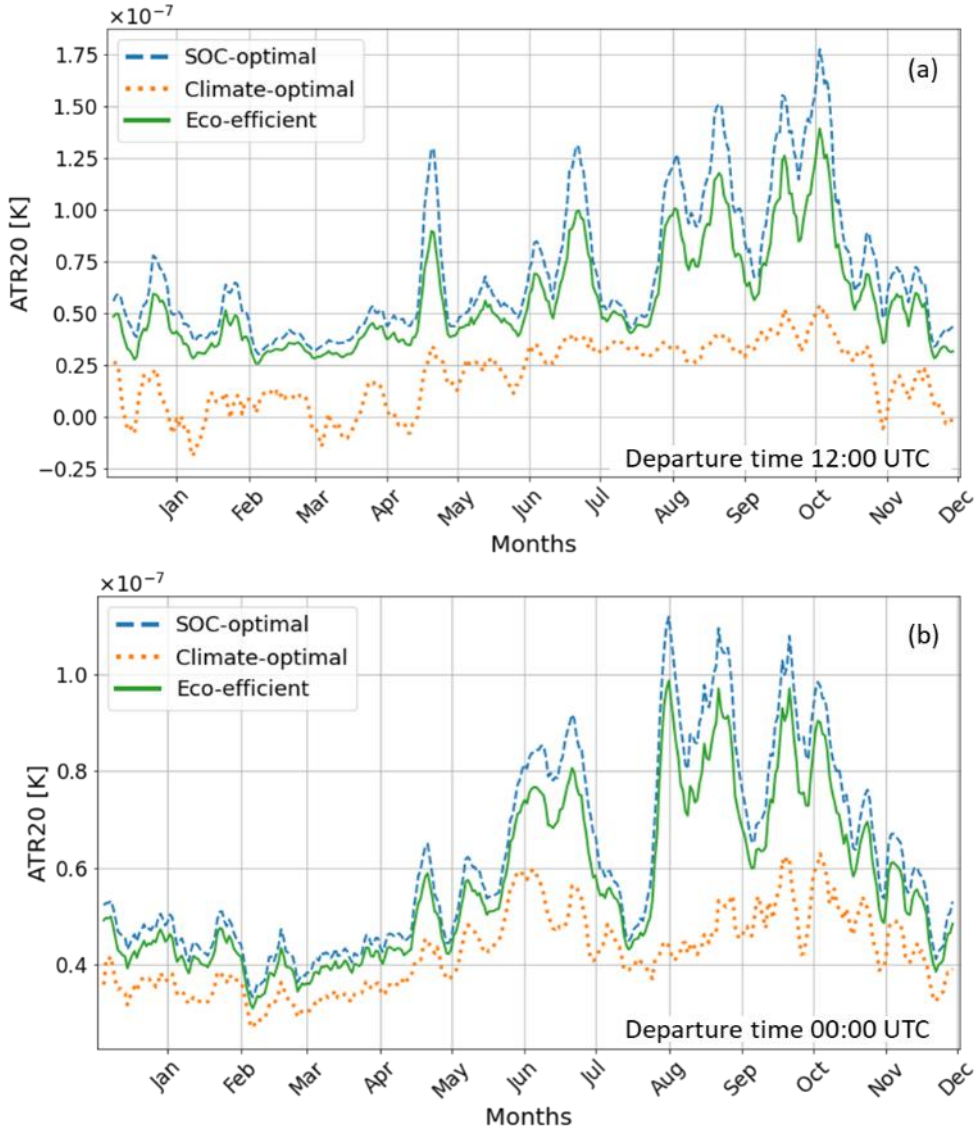

Figure 14 - Variability over time of the total F-ATR20 [K] in 2018 from our air traffic sample. Panels (a) and (b) show the results for flights departing at 12:00 UTC and 00:00 UTC, respectively.

The relative changes in the total F-ATR20 are shown in Figure 15. One can see that, for day-time flights, the largest relative reduction is achieved during the winter, when cooling effects from contrails are exploited. On the other hand, the opposite seasonal cycle is observed for night-time flights: the largest relative reduction in F-ATR20 is during the summer, when the high peaks in the contrail climate impacts are avoided. Lastly, we can see that the mitigation potential of both day-time and night-time reaches a minimum in July, when (1) the impact from contrail is relatively low, as we can see in Figure 22, (2) the impact from ozone is not reduced by eco-efficient trajectories (Figure 12), and (3) cooling effects from contrails are not exploited by the model (Figure 13).

Co-funded by the European Union

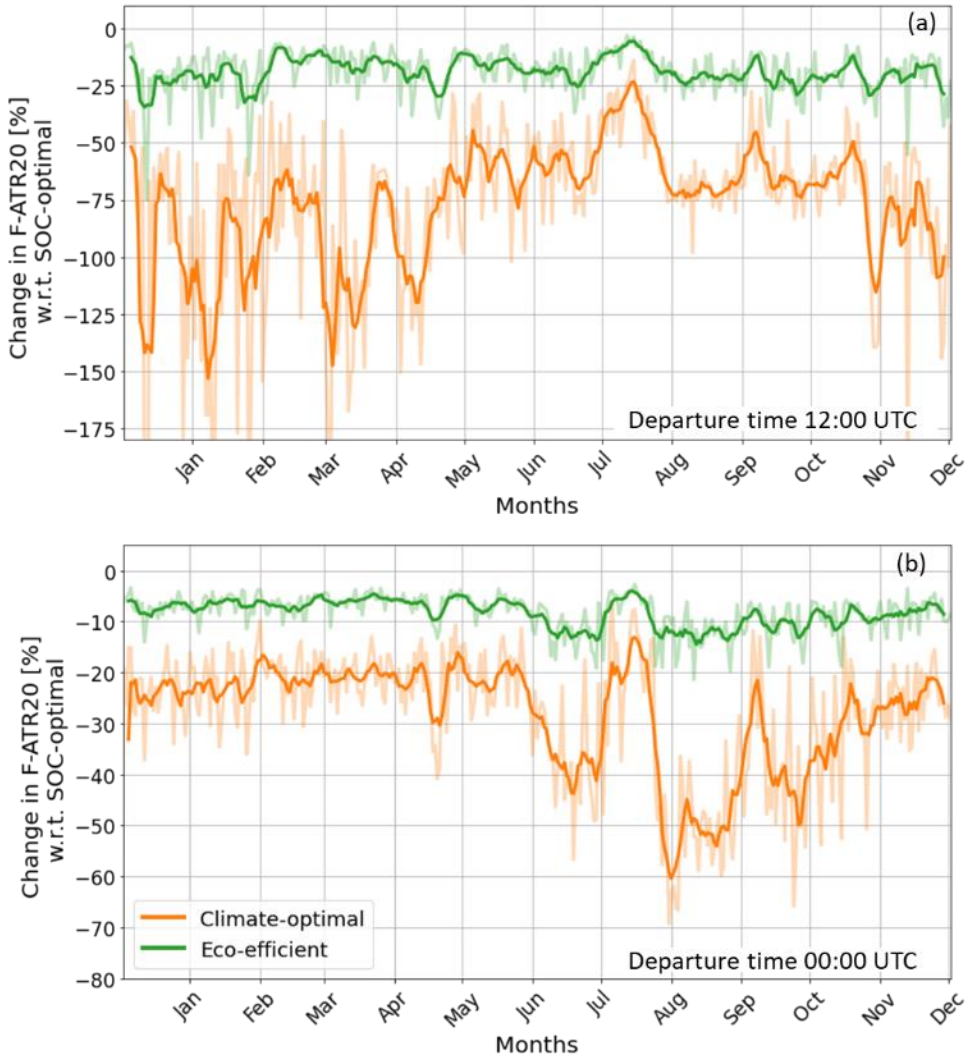

Figure 15 - Relative change [%] in the total F-ATR20 obtained with the climate-optimal (orange) or with eco-efficient (green) trajectories, using as reference the SOC-optimal trajectories. Bold lines: 7-day running average; light curves: daily values. Panels (a) and (b) show the results for flights departing at 12:00 and 00:00 UTC, respectively.

3.1.5 Sensitivity to time horizon

As we have discussed in the previous section, in our simulations, we optimize the trajectories with respect to their climate impact, which is measured in terms of F-ATR20. Here, we consider if our climate-optimal and eco-efficient trajectories are also reducing the climate impact when a longer time horizon (100 years) is taken into account. Therefore, we convert our F-ATR20 values to a different metric, i.e., F-ATR100. The results are shown in Figure 16: one can see that optimizing the trajectories with the F-ATR20 as an objective, the climate impact is also reduced in terms of F-ATR100. This demonstrates that the reduction in short-term climate effects from aviation, such as contrail effects, is also relevant on longer time horizons.

Co-funded by the European Union

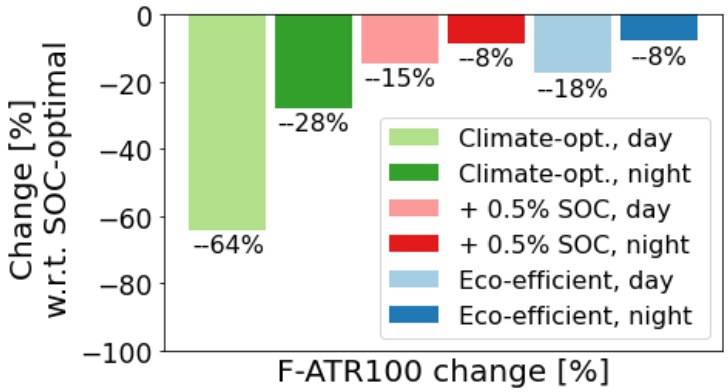

Figure 16 - Relative changes [%] in F-ATR100 with respect to SOC-optimal trajectories.

3.1.6 Focus on 20% of eco-efficient flights with largest F-ATR20 reduction

To quantify and compare the "eco-efficiency" of day-time and night-time optimal flights or of different optimization strategies, we use the climate-cost coefficient k [$/K], which is defined as the increase in cost attributed to per Kelvin reduction in F-ATR20 [17]; in mathematical terms:

$$k = \frac{SOC_x - SOC_{cost-opt}}{ATR20_{cost-opt} - ATR20_x} \left[\frac{\$}{K}\right] \quad (1)$$

where x represents a trajectory optimization strategy – so that the SOC_x and $ATR20_x$ values can refer, for example, to climate-optimal, or eco-efficient solutions, while $SOC_{cost-opt}$ and $ATR20_{cost-opt}$ refer to the reference, climate-optimal scenario.

Table 3 illustrates the values of k [$/K] that are achieved under different optimization strategies. The table compares three optimization strategies (climate-optimal, +0.5% SOC, and eco-efficient), and one additional set of solutions, the top 20% eco-efficient flights: these are the eco-efficient flights leading to the largest absolute changes in F-ATR20.

Climate-cost coefficient k [$/K]							
Climate-optimal		+0.5% SOC		Eco-efficient		Top 20% Eco-eff.	
day-time	night-time	day-time	night-time	day-time	night-time	day-time	night-time
6.645e+11	1.417e+12	2.812e+11	5.392e+11	2.710e+11	5.005e+11	1.506e+11	2.418e+11

Table 3 – Values of the climate-cost coefficient *k* [$/K], under different optimization scenarios, or different departure times (12:00 UTC for day-time flights, 00:00 UTC for night-time flights).

Firstly, we can notice that the day-time values of k [$/K] are lower than the night-time ones under all optimization strategies. This indicates that eco-efficient conditions are more likely to be found for flights departing at 12:00 UTC. Moreover, as expected, the eco-efficient trajectories lead to lower k [$/K] values than the climate optimal trajectories. In other words, for the same reduction rate in F-ATR20, the cost increase in eco-efficient flights is lower compared to the purely climate-optimal flights, which also confirms the effectiveness of the flexible solution-picking algorithm implemented in the new version of AirTraf in identifying the eco-efficient solutions. Furthermore, we can see that such

Co-funded by the European Union

eco-efficient trajectories lead to a SOC increase of about +0.5%. For this reason, a fixed SOC increase of +0.5% was also chosen as trade-off strategy: in fact, this choice allows us to verify if a flexible solution-picking strategy leads to a higher eco-efficiency than a fixed strategy. Indeed, we obtained lower values of the climate-cost coefficient *k* [$/K] in the eco-efficient scenario. On the other hand, a much larger reduction of *k* was obtained when we considered only the top 20% of the total 36600 eco-efficient flights. Therefore, to limit the cost penalty induced by this climate impact mitigation approach, one could focus on a fraction of the flights. More analyses are being conducted to evaluate the mitigation gain in this aspect. For example, the seasonal cycle described in Figure 10 is no longer evident when the top 20% eco-efficient flights are considered (Figure 17, blue curve), but large day-to-day variations still exist. Therefore, the next research step should focus on exploring a possible correlation between specific daily patterns and a high potential for eco-efficiency, with a higher resolution than the seasonal cycle shown in Figure 10.

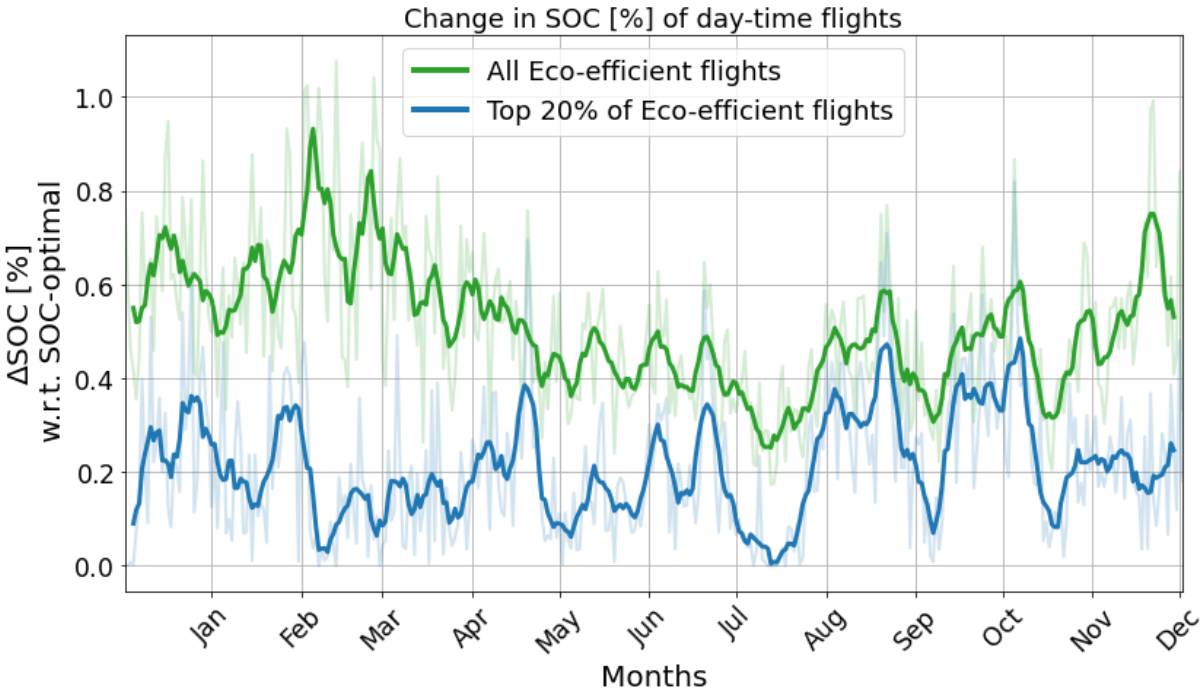

Figure 17 – Relative change [%] in the total SOC obtained with all (green) or the top 20% (blue) eco-efficient trajectories, using as reference the SOC-optimal trajectories. Bold lines: 7-day running average; light curves: daily values. All flights depart at 12:00 UTC.

Figure 18 illustrates the reason for the different *k* [$/K] values obtained considering all the eco-efficient flights, and only the top 20% (Table 3). We observe that the top 20% of eco-efficient flights are responsible for the main fraction (about 70%) of the total reduction in F-ATR20, while their increase in SOC is about 40% of the total.

EUROPEAN PARTNERSHIP

Co-funded by the European Union

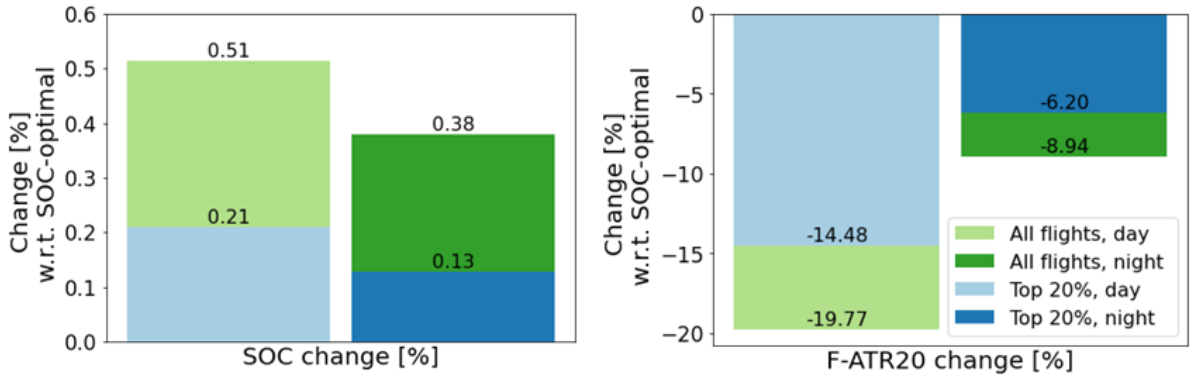

Figure 18 - Relative changes [%] in SOC and F-ATR20 between eco-efficient and SOC-optimal trajectories, comparing the contribution of the top 20% of the eco-efficient flights (blue) with the total changes.

3.2 "Win-win" solutions

"Win-win" solutions are continuously optimized aircraft trajectories that reduce both climate impact as well as operating costs in comparison to the reference case assuming a structured air space. As described in Section 2.2, "win-win" solutions are determined by comparing the optimisation results of ROOST (structured airspace) and TOM (continuous optimization).

For this comparison, the Pareto fronts (from cost optimal solutions to minimum climate solutions) of nine routes have been estimated with ROOST and TOM for the 1st ensemble weather forecast of 5th December, 2018, 00:00 UTC and the associated algorithmic climate change functions assuming harmonised boundary conditions which ensure the comparability of results according to Section 2.2. The points of both Pareto fronts (costs and climate impact) are normalized with respect to the minimum cost trajectory of the structured airspace simulation (red circles in Figure 19).

As indicated in Figure 19 (a)-(i), "win-win" solutions have been identified for all nine investigated routes (grey shaded area). Continuously optimized trajectories show the potential to reduce the costs at a given climate impact between around 2.5% (a) and 7% (g), which reflects the inefficiencies caused by the route structure. At the reference cost level, the climate impact can be reduced between 15% (b) and up to 80% (i) for the investigated routes by assuming free route airspace. However, these large mitigation gains and cost reductions might not be feasible in real world operations due to congestion of airspace and additional boundary conditions. Nevertheless, the results indicate that a large climate impact reduction potential might be associated with the allowance of more flexibility when using the airspace, especially with regard to altitude changes.

EUROPEAN PARTNERSHIP
Co-funded by the European Union

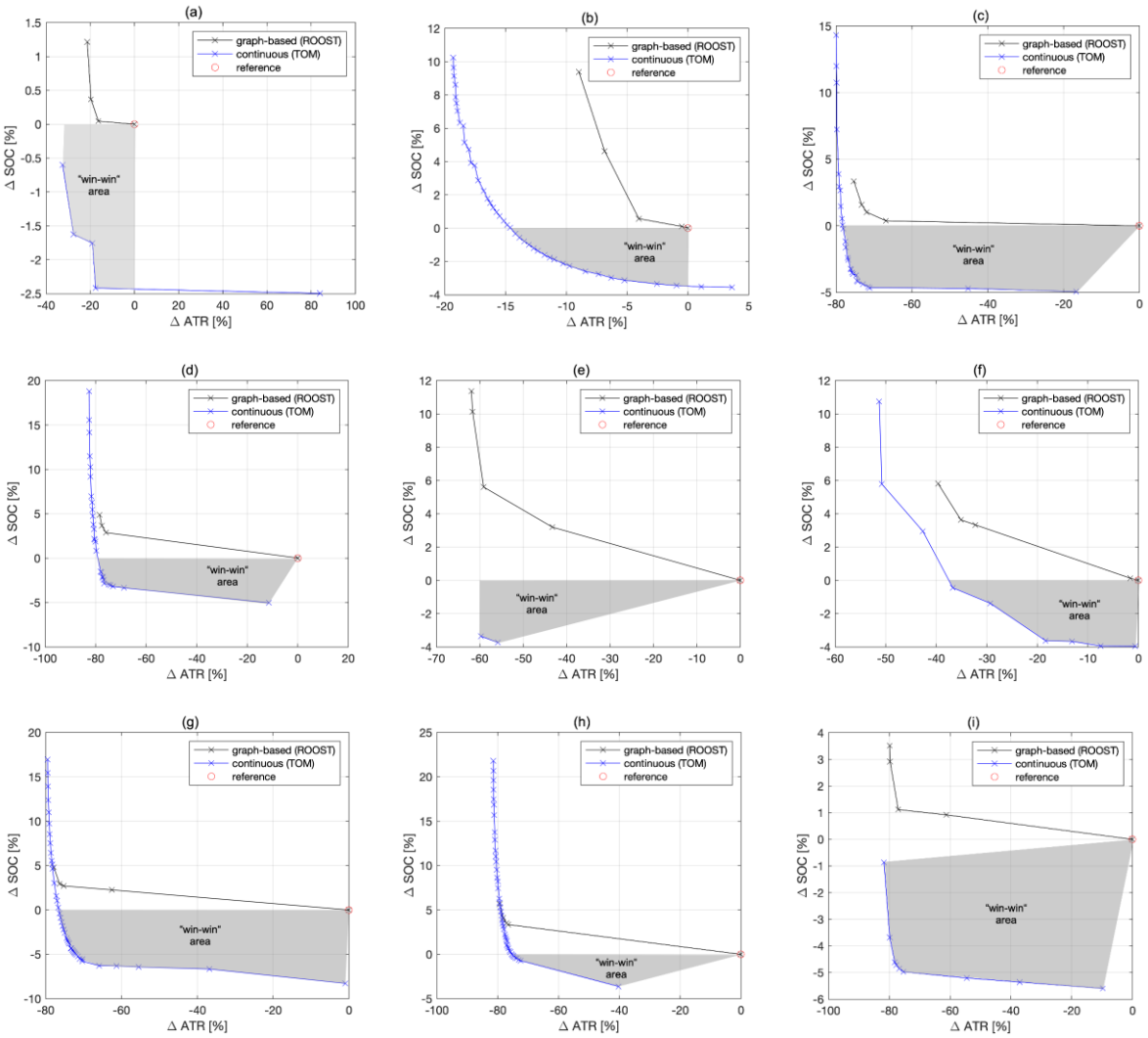

Figure 19 – Pareto-fronts for the routes LTFM-EGLL (a), GCXO-LEMD (b), LFPO-LPPT (c), LEMD-EGLL (d), EHAM-LTFM (e), EGLL-LGAV (f), EHAM-LEBL (g), LEMD-EDDF (h), EHAM-LPPT (i) on 5th December, 2018, 00:00 UTC, 1st ensemble, generated with ROOST (black curves) and TOM (blue curves). The reference point is indicated with a red circle, "win-win" areas are shaded in grey.

Co-funded by the European Union

4 Summary

This report presents the final results found within the WP3 of the FlyATM4E project on “eco-efficient” trajectories, which largely reduce the climate impact of aviation at almost unchanged costs, and on “win-win” situations, which have the potential to reduce both climate impact and operational costs. During this project, the following tasks have been completed:

1. We updated and verified the implementation of the educated guess prototype aCCFs in the ACCF submodel of EMAC;
2. We implemented a new Multi-Objective Optimization Module, including Decision-Making methods, in the AirTraf submodel of EMAC;
3. Using the resulting model system, we conducted annual simulations between December 2017 and December 2018.

These tasks confirmed the possibility of using the EMAC model, coupled with the ACCF and AirTraf submodels, to optimize flight trajectories under a multitude of weather patterns. The optimization can take into account more than one objective function and select a single trade-off solution that best fits the preferences of the decision maker. In this report, we exemplified these model capabilities: the model was able to solve a bi-objective optimization problem, which (1) considered both SOC and total F-ATR20 as objective functions, and (2) selected eco-efficient solutions, which were compared to those trade-off options leading to a fixed +0.5% increase in SOC.

The final results on eco-efficient trajectories are summarised in the following key points:

- Comparing eco-efficient and cost-optimal trajectories, we found that an increase of about 0.5% in operating costs allows reducing the climate impact of day-time flights by about 20%, and the impact of night-time flights by about 10%, in terms of F-ATR20.
- A seasonal cycle in the flight altitudes and SOC changes was found comparing climate-optimal and cost-optimal trajectories, with lower altitudes / higher SOC increases in winter than in summer.
- Changes in contrail effects provide the largest contribution to the reduction in climate impact almost every day and night – with some exceptions in winter when the reduction in the ATR20 from NO_x-ozone is also contributing.
- Optimizing the trajectories including the F-ATR20 in the objective function, the climate impact is also reduced in terms of F-ATR100: therefore, the reduction in short-term climate effects from aviation, such as contrail effects, is also relevant on longer time horizons.

With regard to the “win-win” solutions, the following key statements can be made:

- For the investigated routes and weather situation, at the same level of climate impact, cost reductions between 2.5% and 7% were observed.

EUROPEAN PARTNERSHIP

Co-funded by the European Union

- For the investigated routes and weather situation, at the same level of cost, climate impact reductions between 15% and 80% were observed.
- The large climate impact reductions are essentially driven by adapted altitude profiles.

In this project, a set of prototype aCCFs was employed to estimate the climate impact of aviation (see also D1.2 [28]). On-going research is analysing and expanding these formulas, since their current version has been developed considering a limited temporal and spatial domain (i.e., on representative winter and summer weather patterns, over the North Atlantic flight Corridor). Using these prototype aCCFs, we found that changes in contrail climate impact play the main role in the mitigation potential of trajectory optimization. As cooling effects from contrails were exploited by the model to reduce the total ATR20, especially during winter, the next step in this investigation should explore how our results change when we exclude the possibility of using net negative radiating forcing from contrails in the optimization process. Moreover, as a large daily variability in the mitigation potential was found, the large amount of data collected during this project can be used in future research to investigate if a correlation exists between specific daily weather patterns and the high potential for eco-efficiency. Lastly, we found that the cost penalties of optimizing the aircraft trajectories with respect to their climate impact can be reduced, considering the mitigation potential of the whole air traffic sample, and mitigating the fraction of the flights with the largest potential reduction in ATR20. In other words, a systemic approach to trajectory optimization can be taken into account in the future using ‘a priori’ information (e.g., target absolute reduction in climate impact, determined from the results of this project) as input for our optimization tools.

EUROPEAN PARTNERSHIP

Co-funded by the European Union

5 References

[1] Burris M. A., “Cost index estimation,” in IATA 3rd Airline Cost Conference, Geneva, Switzerland, 2015, p. 1–23.

[2] Dahlmann K., V. Grewe, C. Frömming, U. Burkhardt, “Can we reliably assess climate mitigation options for air traffic scenarios despite large uncertainties in atmospheric processes?,” Transportation Research Part D: Transport and Environment, Volume 46, 2016, Pages 40-55, https://doi.org/10.1016/j.trd.2016.03.006.

[3] Dee D. P., S. M. Uppala, A. J. Simmons, P. Berrisford, P. Poli, S. Kobayashi, U. Andrae, M. A. Balmaseda, G. Balsamo, P. Bauer, P. Bechtold, A. C. M. Beljaars, L. van de Berg, J. Bidlot, N. Bormann, C. Delsol, R. Dragani, M. Fuentes, A. J. Geer, L. Haimberger, S. B. Healy, H. Hersbach, E. V. Hólm, L. Isaksen, P. Kållberg, M. Köhler, M. Matricardi, A. P. McNally, B. M. Monge-Sanz, J.-J. Morcrette, B.-K. Park, C. Peubey, P. de Rosnay, C. Tavolato, J.-N. Thépaut, and F. Vitart, “The ERA-Interim reanalysis: configuration and performance of the data assimilation system,” Quarterly Journal of the Royal Meteorological Society, vol. 137, no. 656, pp. 553–597, apr 2011.

[4] DuBois, D.; Paynter, G.: ‘Fuel Flow Method 2’ for Estimating Aircraft Emissions. In: Society of Automotive Engineers (SAE), SAE Technical Paper 2006-01-1987, 2006.

[5] Frömming C., V. Grewe, S. Brinkop, and P. Jöckel, “Documentation of the EMAC submodels AIRTRAC 1.0 and CONTRAIL 1.0, supplementary material of Grewe et al., 2014b, 7, 175–201,” GMD, 2014.

[6] González-Arribas, D., Jardines, A., Soler, M., García-Heras, J., & Andrés-Enderiz, E., . Probabilistic 4D Flight Planning in Structured Airspaces through Parallelized Simulation on GPUs. International Conference for Research in Air Transportation (ICRAT) 2020

[7] Grewe V., and A. Stenke, “AirClim: An efficient tool for climate evaluation of aircraft technology,” Atmospheric Chemistry and Physics, 2008.

[8] Grewe, V., Champougny, T., Matthes, S., Frömming, C., Brinkop, S., Søvde, O. A., . . . Halscheidt, L. (2014). Reduction of the air traffic’s contribution to climate change: A REACT4C case study. Atmospheric Environment, 94 , 616–625. doi: 10.1016/j.atmosenv.2014.05.059

[9] Grewe, V., Frömming, C., Matthes, S., Brinkop, S., Ponater, M., Dietmüller, S., . . . Hullah, P. (2014, 1). Aircraft routing with minimal climate impact: The REACT4C climate cost function modelling approach (V1.0). Geoscientific Model Development, 7 (1), 175–201. doi: 10.5194/gmd-7-175-2014

[10] Jöckel, P., Kerkweg, A., Pozzer, A., Sander, R., Tost, H., Riede, H., Baumgaertner, A., Gromov, S., and Kern, B.: Development cycle 2 of the Modular Earth Submodel System (MESSy2), Geosci. Model Dev., 3, 717–752, https://doi.org/10.5194/gmd-3-717-2010, 2010.

[11] Köhler, M., Rädel, G., Dessens, O., Shine, K., Rogers, H., Wild, O., Pyle, J. (2008). Impact of perturbations of nitrogen oxide emissions from global aviation. Journal of Geophysical Research. 113. 10.1029/2007JD009140. Lee D. S., D. W. Fahey, A. Skowron, M. R. Allen, U. Burkhardt, Q. Chen, S. J. Doherty, S. Freeman, P. M. Forster, J. Fuglestvedt, A. Gettelman, R. R. De León, L. L. Lim, M. T. Lund, R. J. Millar, B. Owen, J. E. Penner, G. Pitari, M. J. Prather, R. Sausen, and L. J. Wilcox, "The contribution of global aviation to anthropogenic climate forcing for 2000 to 2018," Atmospheric Environment, vol. 244, 2021.

[13] Lee, D. S., D. W. Fahey, A. Skowron, M. R. Allen, U. Burkhardt, Q. Chen, S. J. Doherty, S. Freeman, P. M. Forster, J. Fuglestvedt, A. Gettelman, R. R. De León, L. L. Lim, M. T. Lund, R. J. Millar, B. Owen, J. E. Penner, G. Pitari, M. J. Prather, R. Sausen and L. J. Wilcox (2021). "The contribution of global aviation to anthropogenic climate forcing for 2000 to 2018." Atmospheric Environment: 117834.DOI: https://doi.org/10.1016/j.atmosenv.2020.117834.

[14] Lührs, B.; Niklaß, M.; Frömming, C.; Grewe, V.; Gollnick, V.: Cost-Benefit Assessment of 2D and 3D Climate and Weather Optimized Trajectories. 16th AIAA Aviation Technology, Integration, and Operations Conference (ATIO), 13.-17. June 2016, Washington. DOI: 10.2514/6.2016-3758

[15] Lührs, Benjamin und Linke, Florian und Matthes, Sigrun und Grewe, Volker und Yin, Feijia (2021) Climate Impact Mitigation Potential of European Air Traffic in a Weather Situation with Strong Contrail Formation. Aerospace, 8 (50). Multidisciplinary Digital Publishing Institute (MDPI). doi: 10.3390/aerospace8020050. ISSN 2226-4310.

[16] Matthes S., B. Lührs, K. Dahlmann, V. Grewe, F. Linke, F. Yin, E. Klingaman, and K. P. Shine, "Climate-optimized trajectories and robust mitigation potential: Flying ATM4E," Aerospace, vol. 7, no. 11, pp. 1–15, 2020

[17] Matthes, S., Grewe, V., Dahlmann, K., Frömming, C., Irvine, E., Lim, L., Linke, F., Lührs, B., Owen, B., Shine, K., Stromatas, S., Yamashita, H., & Yin, F. (2017). A concept for multi-criteria environmental assessment of aircraft trajectories. Aerospace, 4(3). https://doi.org/10.3390/aerospace4030042

[18] Nuic, A.; Mouillet, V.: User Manual fort the Base of Aircraft Data (BADA) Family 4. ECC Technical/Scientific Report No. 12/11/22-58, 2012.

[19] Opricovic, S. & Tzeng, G. H. (2004, 7). Compromise solution by MCDM methods: A comparative analysis of VIKOR and TOPSIS. European Journal of Operational Research, 156 (2), 445–455. doi: 10.1016/S0377- 2217(03)00020-1

[20] Roeckner, E., Brokopf, R., Esch, M., Giorgetta, M., Hagemann, S., Kornblueh, L., Manzini, E., Schlese, U., & Schulzweida, U. (2006). Sensitivity of Simulated Climate to Horizontal and Vertical Resolution in the ECHAM5 Atmosphere Model, Journal of Climate, 19(16), 3771-3791.

[21] Simorgh A, Soler M, González-Arribas D, Matthes S, Grewe V, Dietmüller S, Baumann S, Yamashita H, Yin F, Castino F, Linke F, Lührs B, Meuser MM. A Comprehensive Survey on

Climate Optimal Aircraft Trajectory Planning. Aerospace. 2022; 9(3):146. https://doi.org/10.3390/aerospace9030146

[22] Simorgh, A. Soler, M., González-Arribas, D., Matthes, S., Grewe, V., Dietmüller, S., ... & Meuser, M. M. (2022). Robust 4D path planning in structured airspace for the benefit of environment using parallelized simulation on GPUs . Geoscientific Model Development (In preparation).

[23] Wang, Z. & Rangaiah, G. P. (2017, 1). Application and Analysis of Methods for Selecting an Optimal Solution from the Pareto-Optimal Front obtained by Multi-objective Optimization. Industrial and Engineering Chemistry Research, 56 (2), 560–574. doi: 10.1021/acs.iecr.6b03453

[24] Yamashita H., F. Castino, F. Yin, S. Matthes, V. Grewe, S. Dietmüller, P. Jöckel, and P. Rao, "Multi-objective flight trajectory optimization in EMAC: AirTraf 3.0," in preparation, Geoscientific Model Development, 2022.

[25] Yamashita H., F. Yin, V. Grewe, P. Jöckel, S. Matthes, B. Kern, K. Dahlmann, and C. Frömming, "Newly developed aircraft routing options for air traffic simulation in the chemistry–climate model EMAC 2.53: AirTraf 2.0," GMD, vol. 13, no. 10, pp. 4869–4890, 10 2020.

[26] Yin F., V. Grewe, F. Castino, P. Rao, S. Matthes, H. Yamashita, K. Dahlmann, C. Frömming, S. Dietmüller, P. Peter, E. Klingaman, K. Shine, B. Lührs, and F. Linke, "Predicting the climate impact of aviation for en-route emissions: The algorithmic climate change function sub model ACCF 1.0 of EMAC 2.53," in preparation, GMD, 2022.

[27] Yin F., V. Grewe, F. Christine, and Y. Hiroshi. (2018). Impact on flight trajectory characteristics when avoiding the formation of persistent contrails for transatlantic flights. Transportation Research Part D Transport and Environment. 65. 10.1016/j.trd.2018.09.017.

[28] FlyATM4E Deliverable D1.2, 2022: Report on expanded aCCFs including robustness and eco-efficiency aspect

[29] FlyATM4E Deliverable D2.2, 2022: Report on results and assessments of the robustness of eco-efficient trajectories

Appendix A VIKOR method

The VIKOR method is a Multi-Criteria Decision-Making process, which can be employed to identify a recommended solution, taking into consideration the preferences of the decision maker. This is achieved by evaluating the distances of each Pareto-optimal solution from the Positive (Negative) Ideal Solution, having as coordinates the minimum (maximum) feasible values of each objective [19]. In mathematical terms, the following values are determined:

$$f_i^{PI} = \min_j f_{ij}, f_i^{NI} = \max_j f_{ij}$$

where $f_{ij}, i = 1, 2, .. n, j = 1, 2, .. m$ indicates the values of the n objective functions that we want to minimize, for each of the m Pareto-optimal solutions.

These ideal points are used as reference to evaluate the following quantities:

$$S_j = \sum_{i=1}^{n} w_i \left(\frac{f_i^{PI} - f_{ij}}{f_i^{PI} - f_i^{NI}} \right)$$

$$R_j = \max_i \left[w_i \frac{f_i^{PI} - f_{ij}}{f_i^{PI} - f_i^{NI}} \right]$$

$$Q_j = \gamma \frac{S_j - \min_j S_j}{\max_j S_j - \min_j S_j} - (1 - \gamma) \frac{R_j - \min_j R_j}{\max_j R_j - \min_j R_j}$$

where w_i sets the weight of each objective, and $\gamma \in [0, 1]$ represents the weight of maximum group utility. The quantities S_j and R_j represent, respectively, the group utility and individual regret of each point along the Pareto front. The two concepts are summarized by the definition of a third quantity Q_j. Once the values Q_j are computed, the algorithm sorts the set of Pareto-optimal solutions based on their $S_j, R_j,$ and Q_j. Starting from solution x_1, having the lowest Q_j, the following criteria are considered:

- *acceptable advantage*, in which the model computes the difference $Q(x_2) - Q(x_1)$ and recommends the solution x_1 if the result is larger than $\frac{1}{m-1}$. If the condition is not verified, the solutions $x_1, x_2, .. x_l$ are equally recommended, where l is defined as the largest value for which the following is true:

$$Q(x_2) - Q(x_1) \leq \frac{1}{m-1}$$

- *acceptable stability*, in which the model considers if the solution x_1 is the best ranked also with respect to S and R. If not, both x_1 and x_2 are recommended.

As a result, the set of recommended solutions $x_1, x_2, .. x_l$ is identified. If $l > 1$, an additional criterion is chosen to select one solution among the set of recommended solutions. In our implementation

EUROPEAN PARTNERSHIP

Co-funded by the European Union

within the AirTraf model, the method selects the solutions corresponding to the minimum value of one of the two objectives.

EUROPEAN PARTNERSHIP

Co-funded by the European Union

Appendix B Additional figures

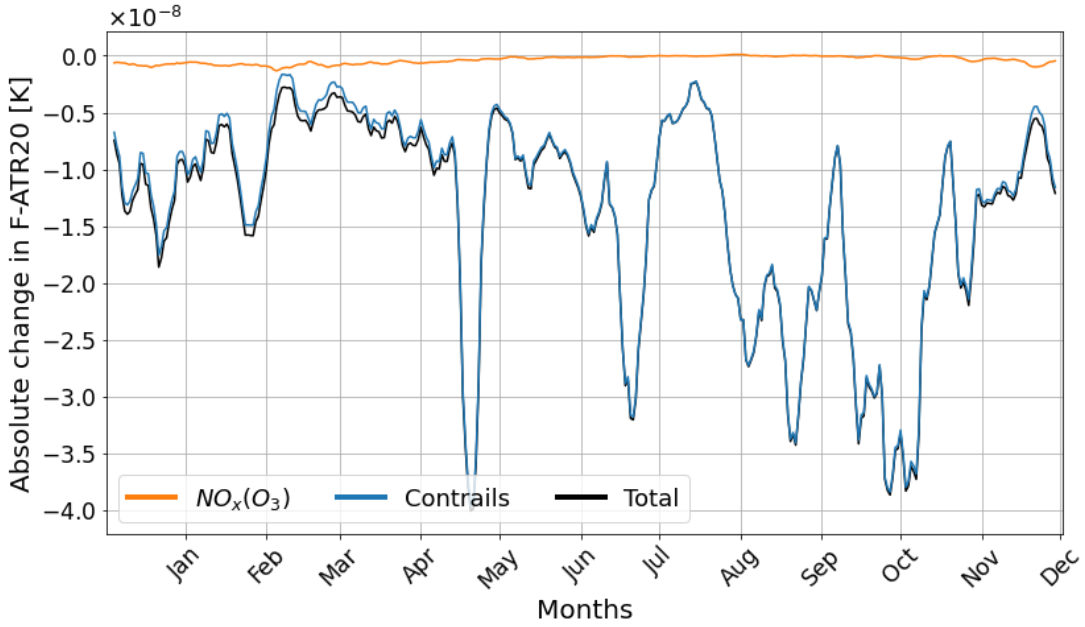

Figure 20 – Difference in the total F-ATR20 [K] of eco-efficient and cost-optimal trajectories departing at 12:00 UTC, from 1 Dec. 2017 to 1 Dec. 2018. Each colour represents a specific climate effect from aviation emissions. The curves represent 7-days running average values.

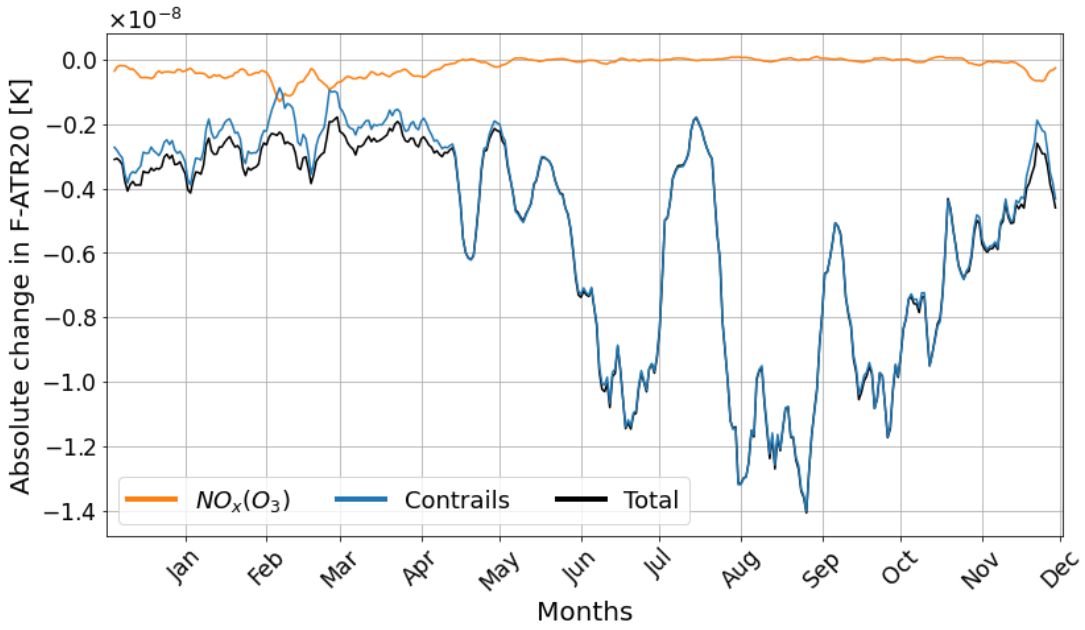

Figure 21 - Difference in the total F-ATR20 [K] of eco-efficient and cost-optimal trajectories departing at 00:00 UTC, from 1 Dec. 2017 to 1 Dec. 2018. Each colour represents a specific climate effect from aviation emissions. The curves represent 7-days running average values.

EUROPEAN PARTNERSHIP

Co-funded by the European Union

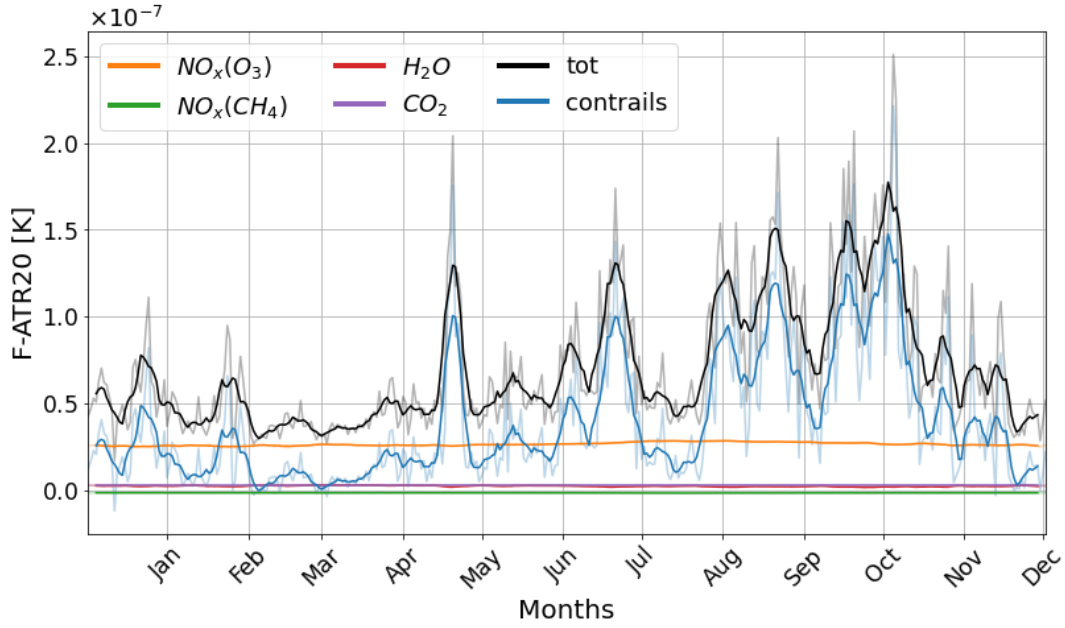

Figure 22 - Evolution in time of the total F-ATR20 [K] of cost-optimal trajectories departing at 12:00 UTC, from 1 Dec. 2017 to 1 Dec. 2018. Each colour represents a specific climate effect from aviation emissions. Bold lines: 7-days running average; lighter curves: daily values.

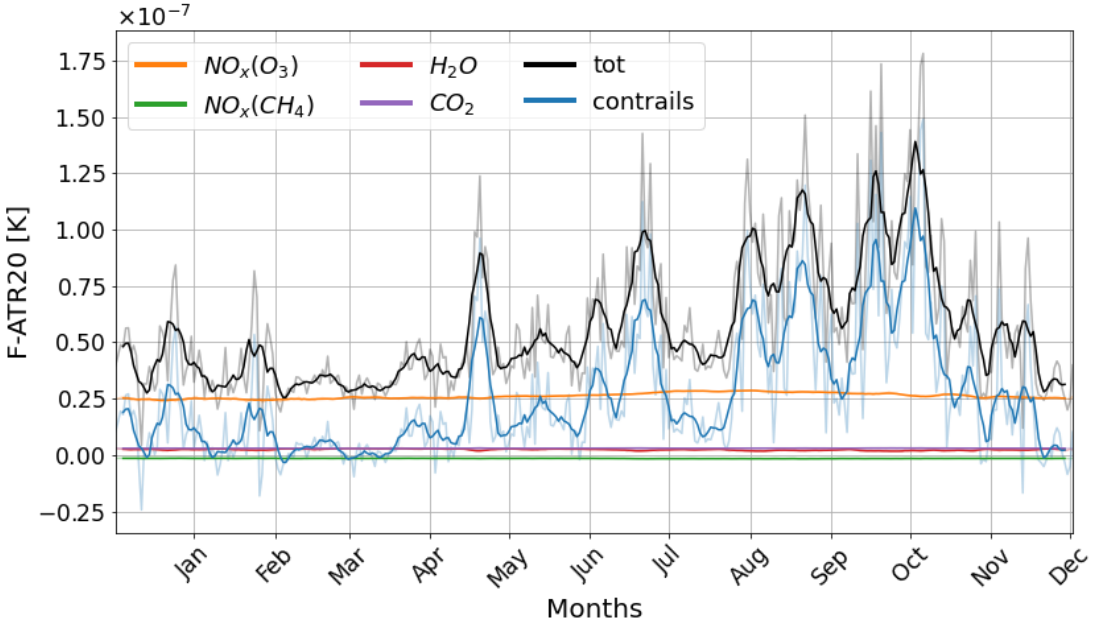

Figure 23 - Evolution in time of the total F-ATR20 [K] of eco-efficient trajectories departing at 12:00 UTC, from 1 Dec. 2017 to 1 Dec. 2018. Each colour represents a specific climate effect from aviation emissions. Bold lines: 7-days running average; lighter curves: daily values.

EUROPEAN PARTNERSHIP

Co-funded by the European Union

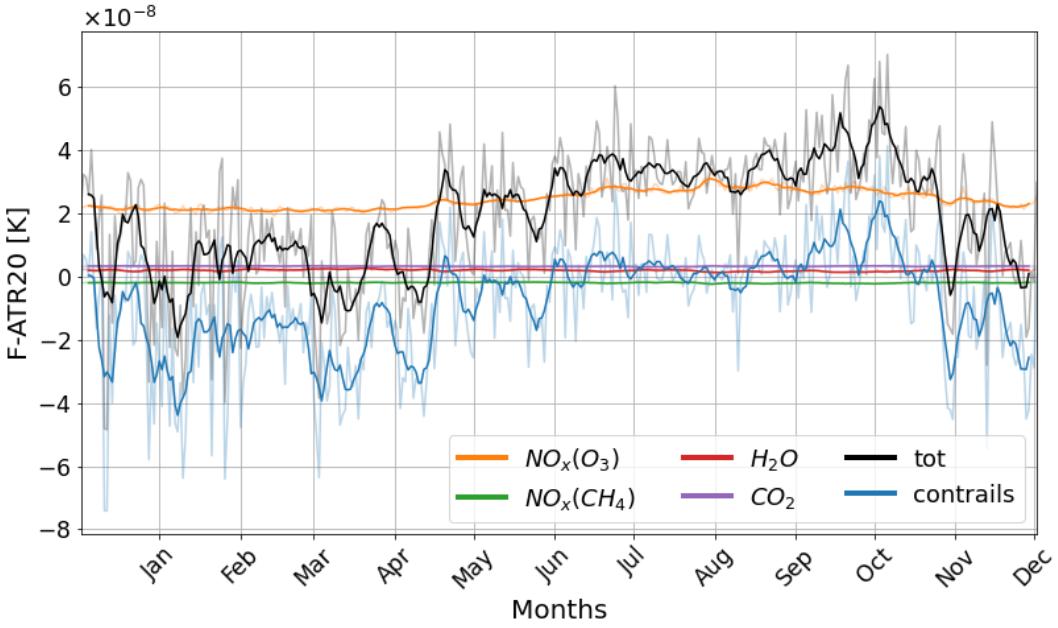

Figure 24 - Evolution in time of the total F-ATR20 [K] of climate-optimal trajectories departing at 12:00 UTC, from 1 Dec. 2017 to 1 Dec. 2018. Each colour represents a specific climate effect from aviation emissions. Bold lines: 7-days running average; lighter curves: daily values.

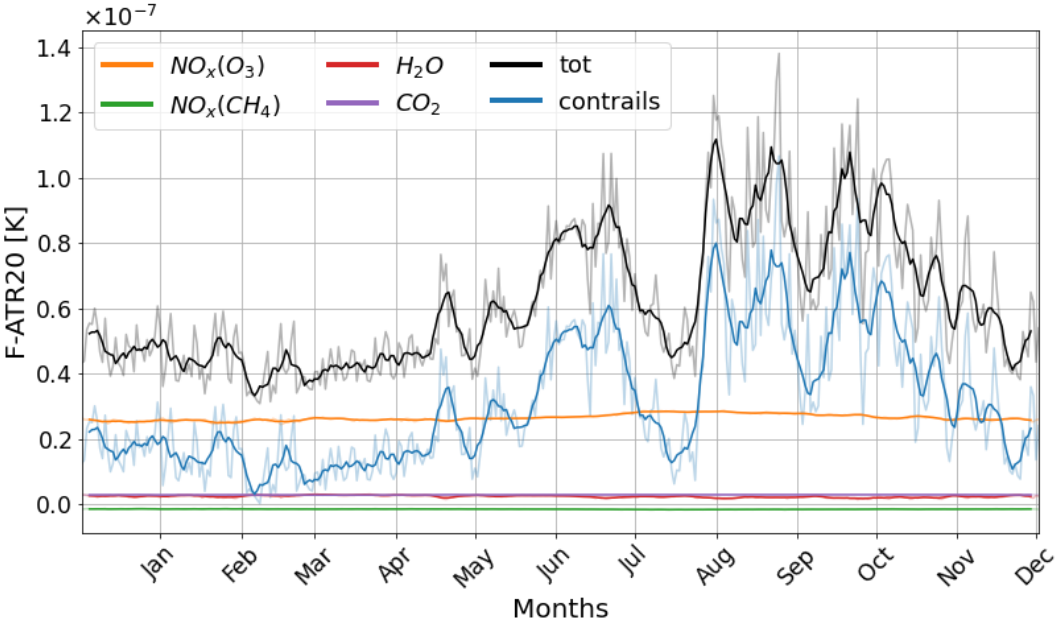

Figure 25 - Evolution in time of the total F-ATR20 [K] of cost-optimal trajectories departing at 00:00 UTC, from 1 Dec. 2017 to 1 Dec. 2018. Each colour represents a specific climate effect from aviation emissions. Bold lines: 7-days running average; lighter curves: daily values.

Co-funded by the European Union

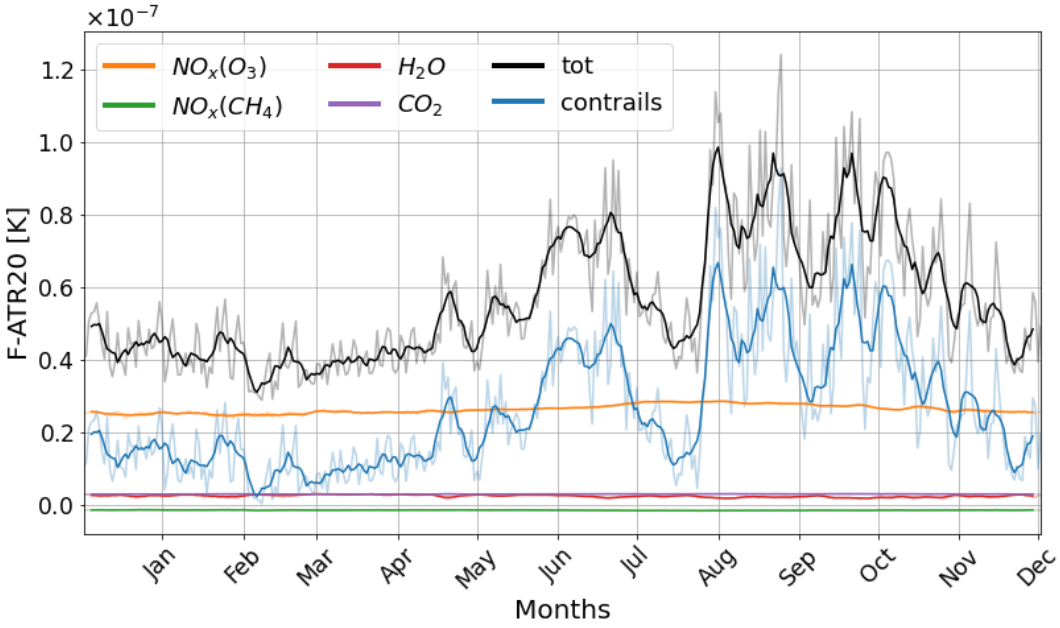

Figure 26 - Evolution in time of the total F-ATR20 [K] of eco-efficient trajectories departing at 00:00 UTC, from 1 Dec. 2017 to 1 Dec. 2018. Each colour represents a specific climate effect from aviation emissions. Bold lines: 7-days running average; lighter curves: daily values.

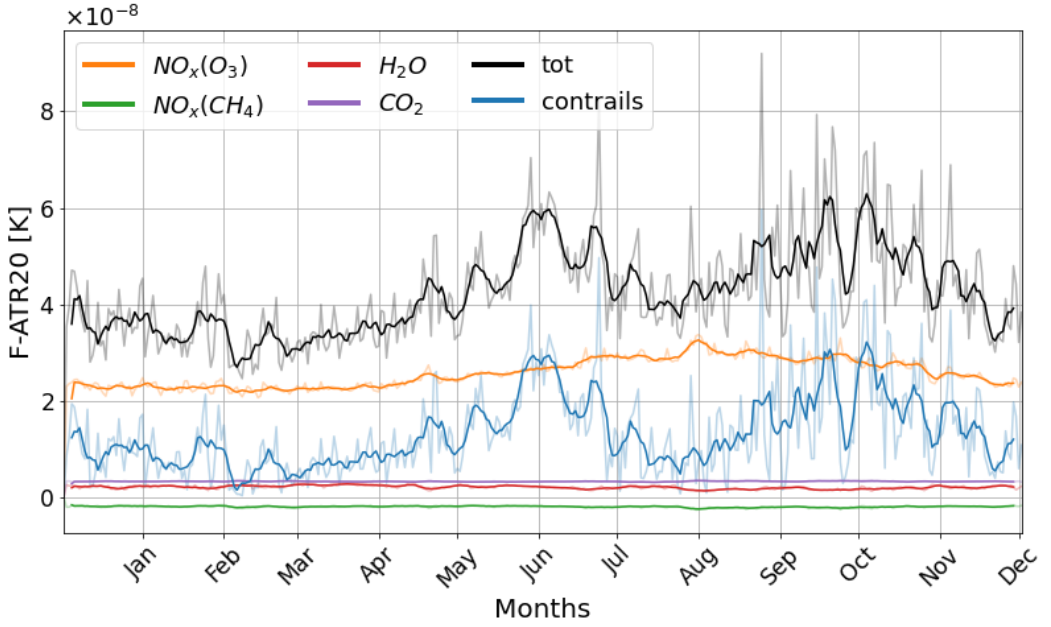

Figure 27 - Evolution in time of the total F-ATR20 [K] of climate-optimal trajectories departing at 00:00 UTC, from 1 Dec. 2017 to 1 Dec. 2018. Each colour represents a specific climate effect from aviation emissions. Bold lines: 7-days running average; lighter curves: daily values.

EUROPEAN PARTNERSHIP

Co-funded by the European Union

Acronyms and FlyATM4E consortium

Table 4: Non-exhaustive list of acronyms used across the text.

Acronym	Description
aCCF	algorithmic climate change functions
AirTraf	Air Traffic simulator
ATM	Air Traffic Management
ATR20	Average temperature response over 20 years
P-ATR20	ATR20 of a Pulse emission
F-ATR20	ATR20 for a BAU emission scenario
BAU	Business As Usual
ECMWF	European Centre for Medium-Range Weather Forecasts
EMAC	ECHAM5/MESSy2 Atmospheric Chemistry Model
NO_x	Nitrogen oxide
ROOST	Robust Optimization Of STructured airspace
SESAR	Single European Sky ATM Research Programme
SID	Standard Instrument Departure
SJU	SESAR Joint Undertaking
SOC	Simple Operating Costs
STAR	Standard Instrument Arrival
TOM	Trajectory Optimization Module
WP	Work Package

Table 5: FlyATM4E consortium acronyms

Acronym	Description
DLR	DEUTSCHES ZENTRUM FUER LUFT - UND RAUMFAHRT EV
TUD	TECHNISCHE UNIVERSITEIT DELFT
TUHH	TECHNISCHE UNIVERSITAT HAMBURG
UC3M	UNIVERSIDAD CARLOS III DE MADRID

EUROPEAN PARTNERSHIP

Co-funded by the European Union

Co-funded by
the European Union